



OPEN Molecular simulation study of adsorption-diffusion of CH₄, CO₂ and H₂O in gas-fat coal

Jinzhang Jia^{1,2}, Yinghuan Xing^{1,2}✉, Bin Li³, Yumo Wu^{1,2} & Dongming Wang^{1,2}

In order to clarify the microscopic dynamics mechanism of CH₄, CO₂ and H₂O adsorption and diffusion in coal, and to reveal the mechanism of the influence of different temperatures and pressures on the adsorption and diffusion characteristics of coal adsorbed CH₄, CO₂ and H₂O molecules. In this paper, the macromolecular structure model of Jixi gas-fat coal was constructed, based on the Giant Canonical Monte Carlo (GCMC) and Molecular Dynamics (MD) methods. The adsorption-diffusion characteristics of CH₄, CO₂ and H₂O single-component gases in the gas-fat coal macromolecule model at temperatures ranging from 273.15 K to 313.15 K and pressures ranging from 0.01 MPa to 15 MPa were investigated by using Material Studio software. The research results indicated that: The adsorption of three gases, CH₄, CO₂ and H₂O, increased with the increase of equilibrium pressure, and the adsorption isotherms conformed to Langmuir type I isotherms. The amount of saturated adsorption of CH₄ ranged from 11.18 to 14.37 ml/g, the saturated adsorption of CO₂ ranged from 20.40 to 24.70 ml/g, and the saturated adsorption of H₂O ranged from 66.61 to 84.21 ml/g. With the increase of temperature, the saturated adsorption of CH₄ and CO₂ both decreased, and the saturated adsorption of H₂O firstly increased and then decreased, and the adsorption of H₂O by low temperature and high temperature had both an inhibitory effect on the adsorption of H₂O. The potential energy distributions of CH₄, CO₂ and H₂O molecules are poisson distributed. The absolute values of the most available interaction energies are, from highest to lowest: H₂O > CO₂ > CH₄; the activation energies for diffusion of CH₄, CO₂ and H₂O are 12.20 kJ/mol, 3.36 kJ/mol, and 8.47 kJ/mol, respectively, and the diffusion of CO₂ is the more likely to occur. The adsorption of CH₄ and CO₂ in coal is physical adsorption, while the adsorption process of H₂O molecules is beyond the scope of physical adsorption. The absolute value of the interaction energy is H₂O > CO₂ > CH₄ in descending order.

Keywords Coal mine gas control, Coal macromolecular modeling, Molecular simulation, Grand canonical Monte Carlo, Adsorption-diffusion

Coal bed methane (CBM) is mainly composed of CH₄ and a small amount of CO, CO₂ and N₂. A large number of experts and scholars have carried out a large number of experimental and simulation studies on the adsorption and diffusion mechanism of CBM in coal to provide theoretical support for the injection of CO₂ and N₂ to promote gas extraction and to improve the efficiency of CBM development.

Liang Bing¹ conducted methane isothermal adsorption experiments on pulverized coal and lump coal using a self-developed experimental platform, and the results showed that pulverized coal has a larger adsorption capacity compared with lump coal, and the smaller the particle size of pulverized coal, the larger the adsorption capacity. Long² investigated the adsorption of CH₄, CO₂ and N₂ in different sizes of microporous structures by molecular simulation, the results indicate that the amount of adsorption in the pore model increases with the increase of the pore size, the heat of adsorption decreases with the increase of the pore size, and the larger the pore size, the more beneficial to the diffusion of the gas, the radius of action between gases and carbon atoms is investigated by using a radial distribution function, and the smallest effective distance between CO₂ and carbon atom is found with the biggest effective radius, and the biggest effective distance between N₂ and carbon atoms is found with the smallest range of action. Lin³ investigated the microscopic adsorption mechanism of CH₄, CO₂ and N₂ single, binary as well as triple components in Wiser bituminous coal by GCMC and MD methods. The result indicated that CO₂ has the highest adsorption capacity and N₂ has the lowest adsorption capacity, and the

¹College of Safety Science and Engineering, Liaoning Technical University, Fuxin 123000, China. ²Key Laboratory of Mine Thermodynamic disasters and Control of Ministry of Education (Liaoning Technical University), Huludao 125105, China. ³School of Environmental and Chemical Engineering, Shenyang Ligong University, Shenyang 110159, China. ✉email: 1436529185@qq.com

adsorption amount increases and the adsorption separation coefficient decreases with the concentration of CO₂ in the binary component. High concentration of CO₂ had a negative effect on competitive adsorption. CO₂ had the strongest interactions in the coal molecule, and the isosteric heat of adsorption was inversely proportional to the molar volume fraction of CO₂. Wu⁴ in order to reveal the microscopic mechanism of the competitive adsorption of CO₂, O₂, and N₂, and to provide theoretical support for injecting coal combustion flue gas into the goaf to effectively store CO₂ and prevent fire. A macromolecular coal model was established, and the competitive adsorption of monomer, binary and ternary was investigated based on the GCMC and MD methods, and the results showed that CO₂ has greater electrostatic and van der Waals energies with coal, and the interaction energy with coal is greater than that of O₂ and N₂, so the adsorption of the three gases is: CO₂ > O₂ > N₂. Mazumder⁵ and Mabuza⁶ et al. investigated the adsorption of flue gases on coal by experimental methods and concluded that CO₂ is the optimal adsorption component. Wu⁷ investigated the micro-mechanisms of CO₂ storage and CH₄ recovery during flue gas injection into coal beds in a coal-fired power plant, established dry and wet coal macromolecular models, and investigated the mono- and multivariate adsorption between flue gas and CH₄. The results indicate that the adsorption of mixed gases in coal is related to the physical properties of the individual gases themselves on the one hand, and affected by the gas molar fraction on the other. As the preferential adsorption sites are occupied by water, the moisture in coal is unfavorable to the adsorption of gases, and the effect on CO₂ is particularly obvious. Kurniawa⁸ investigated the adsorption behavior of multicomponent gases in coal by GCMC method and confirmed that CO₂ is more easily adsorbed on coal molecules than N₂ and CH₄. Asif⁹ investigated the competing adsorption behavior of CO₂ and CH₄ on different coal ranks, and the results of the research indicated that: the competing adsorption capacity of CO₂ increases gradually with the increase of the coal rank, and this is mainly related to the structure of coal's functional groups, fat side chains and other structures. Brochard¹⁰ investigated the effect of different factors on the competitive adsorption of CH₄/CO₂ using numerical simulations, and the results indicated that the selectivity of CH₄/CO₂ adsorption was affected by temperature, gas concentration, pressure and other factors.

Experts and scholars have carried out a large number of experimental and simulation studies on CH₄ and CO₂ adsorption, revealing the competitive adsorption mechanism between coal and CH₄ and CO₂ single and binary components, and scholars have carried out a large number of experimental studies on coal adsorption of water molecules, revealing the adsorption characteristics of water in the coal seam. However, the effect of water molecules on the adsorption characteristics of CH₄ and CO₂ has been less studied, and there have been few studies on the microscopic mechanism of water molecules adsorption in coal, and there is a relative lack of molecular level studies on the adsorption and diffusion characteristics of coal adsorption of CH₄, CO₂, and H₂O molecules at different temperatures and pressures. The aim of this paper is to investigate the adsorption-diffusion behaviors of CH₄, CO₂, and H₂O single-component gases in a gas-fat coal macromolecule model at temperatures ranging from 273.15 K to 313.15 K and pressures ranging from 0.01 MPa to 15 MPa by using the Giant Canonical Monte Carlo (GCMC) and molecular dynamics (MD) methods with Material Studio. Analyze the effects of pressure and temperature on gas adsorption, energy distribution, probability concentration distribution, diffusion coefficient, isosteric heat of adsorption and interaction energy.

Methodology

Molecule model

Coal is a kind of non-homogeneous porous material with complex physical and chemical structure, domestic and foreign experts and scholars use a variety of characterization and testing instruments to analyze the coal macromolecular structure, to obtain all kinds of functional groups and microcrystalline structure information of coal, and construct a large number of models of coal macromolecular structure. Fuchs¹¹ first constructed a coal model in 1942, Given¹² in 1960, 1970 Wisler¹³, 1984 American scholar Shinn¹⁴ have constructed the coal macromolecular structure model, in this paper, using FTIR, XPS, ¹³C-NMR, XPS, industrial, elemental analysis and other test methods, independently constructed the gas-fat coal macromolecule model, the molecular formula (C₂₁₂H₁₈₉O₃₈N₃S), the planar two-dimensional structure shown in Fig. 1.

The two-dimensional planar model of gas-fat coal was imported into MS software, saturated with hydrogen, and geometrically optimized, annealed, and dynamically optimized to finally obtain the macromolecular lowest energy configuration of gas-fat coal. The Amorphous Cell module was used to construct the three-dimensional cell structure of gas-fat coal, and 15 macromolecule minimum energy models of gas-fat coal were put into the cell to add three-dimensional periodic boundaries, and the parameters were set as shown in Table 1, and the molecular dynamics method was used to perform the geometric optimization, annealing optimization, and dynamic optimization on the cell structure of Jixi gas-fat coal to get the minimum energy configuration of the three-dimensional cell structure of Jixi gas-fat coal, as shown in Fig. 2.

The density of gas-fat coal macromolecule cell model is stable at 1.14 g/cm³, and the measured density of Jixi gas-fat coal is 1.17 g/cm³, and the simulated density is slightly lower than the measured value. On the one hand, due to the presence of quartz sand, kaolinite and other non-mineral substances in the coal, on the other hand, there are small molecules of organic matter in the coal macromolecule model, the modeling process does not take into account the non-mineral substances and small molecules of organic matter resulting in the simulated density is lower than the experimental density, it is considered that the gas-fat coal cell structure constructed in this paper is reasonable. The cell structure of Jixi gas-fat coal has the dimensions A = B = C = 4.09543 nm, $\alpha = \beta = \gamma = 90^\circ$, and the molecular formula C₃₁₈₀H₂₈₃₅N₄₅O₅₇₀S₁₅. The microporous distribution characteristics of Jixi gas-fat coal were investigated by using the Atom Volumes & Surfaces module, with the Connolly probe radius of 0.13 nm and the van der Waals' scanning factor of 1.0 Å. The microporous distribution of the model is shown in the following table. Å, the microporous distribution of the model is shown in Fig. 2.

Using Material Studio software to construct CH₄, CO₂ and H₂O molecules, CH₄ is tetrahedron structure, CO₂ is rectilinear triatomic structure, and H₂O is folded triatomic structure, the energy optimization of gas

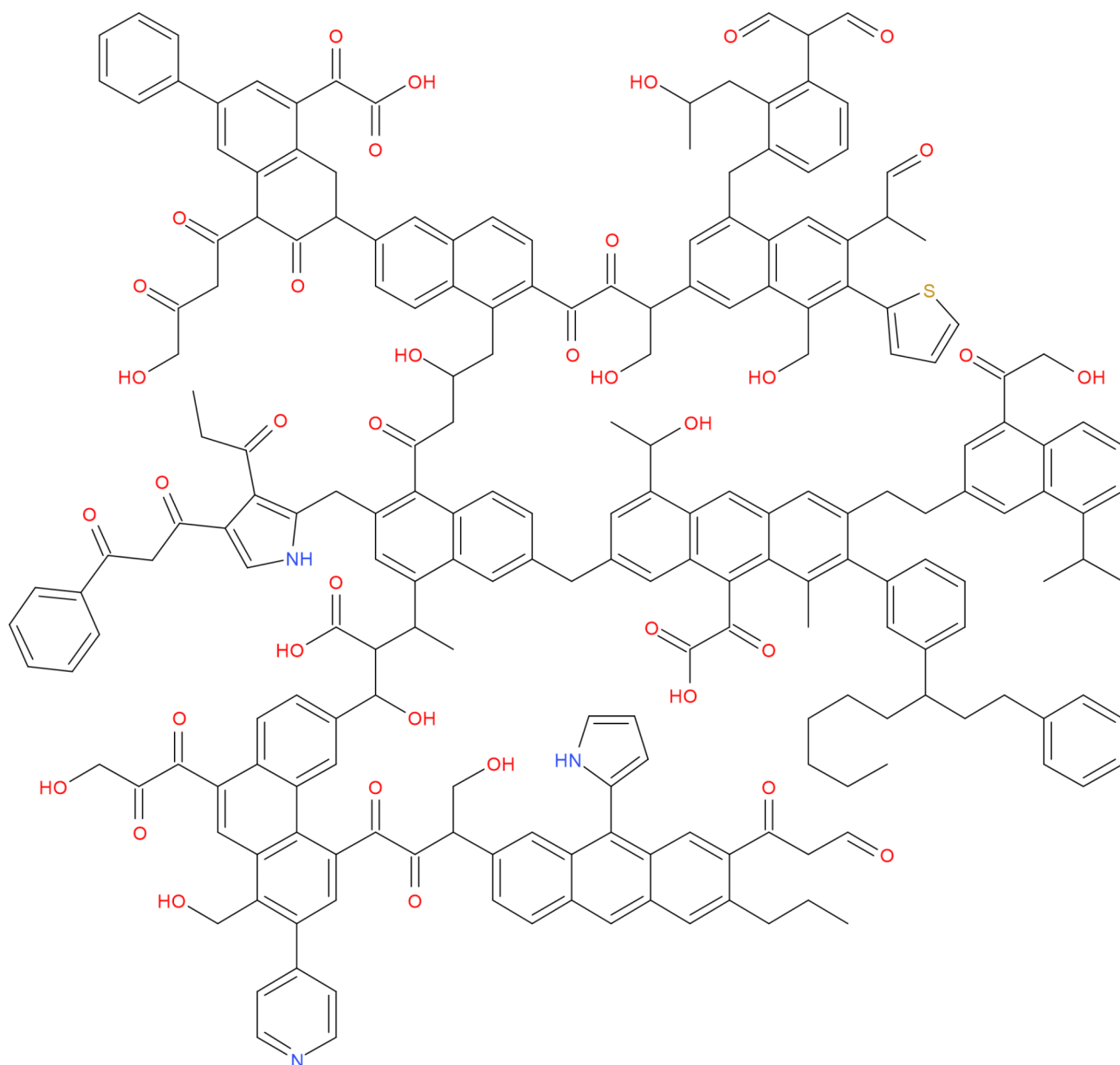


Fig. 1. Planar model of macromolecular structure of gas-fat coal.

Setting	Parameter	Setting	Parameter
Take	Construction	Force field	COMPASS
Quality	Medium	Charges	Forcefield assigned
Density	1.14 g/cm ³	Electrostatic	Atom based
Temperature	298 K	van der Waals	Atom based

Table 1. Density simulation parameters.

small molecule model to get the lowest energy model of CH₄, CO₂ and H₂O molecules, as shown in Fig. 3, the three gas molecules were optimized to get the final energy close to zero, the three adsorbate molecules have a large difference in terms of their physical properties, as shown in Table 2, which is an important reason of the different nature of gas-fat coal adsorbed on them.

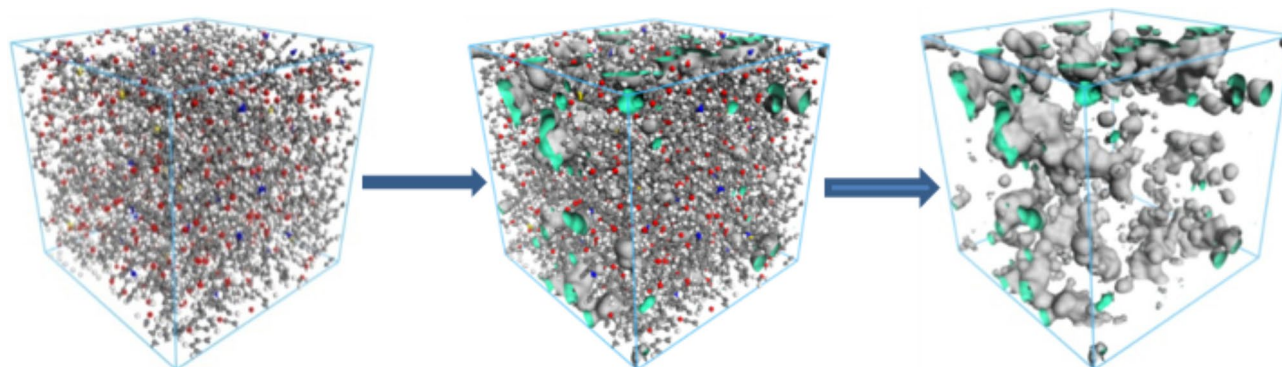


Fig. 2. 3D macromolecular pore characteristics of gas-fat coal.

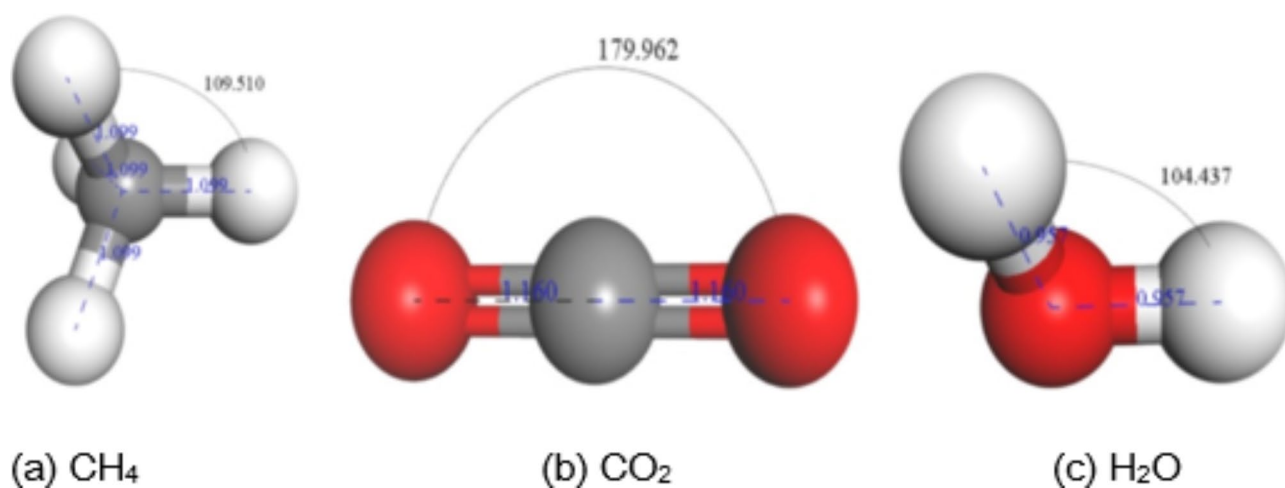


Fig. 3. CH_4 , CO_2 and H_2O small molecule models.

Gas-type	Shape	Boiling/K	Dd	Pr	Dm	Qm	Charge/e		
							C	H	O
CH_4	Tetrahedron	111.65	0.38	2.60	0	0	-0.596	0.149	-
CO_2	Linear	194.65	0.33	2.65	0	4.30	0.892	-	-0.446
H_2O	Folded linear	373.15	0.27	1.48	1.86	9.77	-	0.336	-0.672

Table 2. Physical properties of CH_4 , CO_2 and H_2O . *Dd* dynamic diameter/nm, *Pr* polarization ratio/ 10^{-24}cm^3 , *Dm* dipole moment/ 10^{-18}esu cm , *Qm* quadrupole moment/ 10^{-26}esu cm^2 .

Simulation methodology and parameter setting

The adsorption behavior of CH_4 , CO_2 and H_2O molecules on the macromolecular structural model of Jixi gas-fat coal were investigated based on the Giant Canonical Monte Carlo and molecular dynamics methods. The Sorption module was used, and the parameter settings of the MS software are shown in Table 3.

The adsorption volume (molecules/u.c) obtained from the software simulation was converted to the experimental and engineering adsorption volume (ml/g), which can be expressed as:

$$Q = \frac{N}{M} \quad (1)$$

In formula: *Q* is the gas adsorption amount, mol/g; *N* is the number of adsorbed gases, molecules/u.c; *M* is the molar mass of coal as macromolecules, g/mol;

The relationship between excess adsorption amount and absolute adsorption amount conversion is shown in Eq. (2):

Setting	Parameter	Setting	Parameter
Task	Fixed pressure	Production steps	2×10^7
Quality	Customized	Charges	Forcefield assigned
Forcefield	COMPASS	Electrostatic	Ewald
Equilibration steps	1×10^7	van der Waals	Atom based
Ewald accuracy	0.001 kcal/mol	Cutoff distance	12.5Å
Exchange	0.40	Conformer	0.2
Rotate	0.2	Translate	0.2

Table 3. Adsorption simulation parameter settings.

$$N_{ex} = N_{ab} - N_A PV_v / RT \quad (2)$$

In formula: N_{ex} is the amount of excess adsorption of gas molecules in the coal macromolecular structure, molecules/u.c; N_{ab} is the amount of absolute adsorption of gas molecules in the coal macromolecular structure, molecules/u.c; N_A is Avogadro's constant, which is taken to be 6.02×10^{23} ; and V_v is the pore volume of accessible pores in the coal macromolecular structure, mL.

Converting the excess adsorption of gas molecules adsorbed by the coal macromolecular structure model to the adsorbed amount mL/g at the standard condition can be expressed as:

$$Q_{ex} = 22,400 \times \frac{N_{ex}}{M} \quad (3)$$

In formula: Q_{ex} is the excess adsorption of the modelled coal macromolecular structure, mL/g.

Pressure and fugacity conversion

Material Studio simulation uses fugacity rather than pressure, fugacity can describe the state of motion of an object, usually expressed in terms of the velocity and acceleration of an object, representing the state in which the object is in, and indicates the propulsive force or escape ability of the object to migrate in that state, it was chosen to use the Peng-Robinson¹⁵ equation of state to convert the pressure of a gas to fugacity, as follows:

$$P = \frac{RT}{V-b} - \frac{a(T)}{V(V+b) + b(V-b)} \quad (4)$$

Rewrite Eq. (4) in the form of Eq. (5):

$$Z^3 - (1-B)Z^2 + (A-3B^2-2B)Z - (AB-B^2-B^3) = 0 \quad (5)$$

In formula: Z is the gas compression factor, A and B are the equation coefficients, which can be expressed as:

$$A = \frac{aP}{R^2T^2} \quad (6)$$

$$B = \frac{bP}{RT} \quad (7)$$

$$Z = \frac{PV}{RT} \quad (8)$$

In formula: P is the gas pressure, MPa; R is the gas molar constant; V is the gas molar volume, 22.4 L/mol.

In formula: Eq. (4) has¹⁶ Eqs. (9), (10) at critical points and non-critical points as shown in Eq. (11)

$$a(T_c) = 0.45724 \frac{R^2 T_c^2}{P_c} \quad (9)$$

$$b(T_c) = 0.07780 \frac{RT_c}{P_c} \quad (10)$$

$$a(T) = a(T_c) \cdot a(T_r, \omega) \\ = 0.45724 \frac{R^2 T_c^2}{P_c} \left[1 + (0.37464 + 1.54226\omega - 0.26992\omega^2) \left(1 - \sqrt{\frac{T}{T_c}} \right) \right]^2 \quad (11)$$

$$b(T) = b(T_c) = 0.07780 \frac{RT_c}{P_c} \quad (12)$$

Absorbate	P_c /MPa	T_c /K	w
CH ₄	4.5992	190.56	0.012
CO ₂	7.3773	304.13	0.224
H ₂ O	22.0640	647.10	0.345

Table 4. Thermodynamic parameters of CH₄, CO₂ and H₂O.

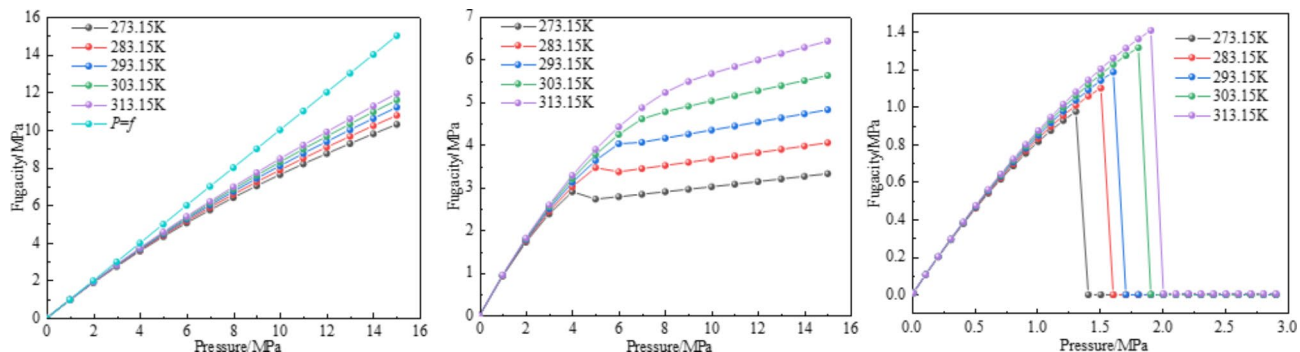


Fig. 4. Fugacity of CH₄, CO₂ and H₂O at different temperatures and pressures.

In formula: T_c is the critical temperature, K; T_r is the contrast temperature, K; P_c is the critical pressure, MPa; ω is the eccentricity factor.

Substituting Eq. (13) into Eq. (4), the expression of fugacity f can be obtained as follows:

$$\ln \frac{f}{P} = \int_0^P \left(\frac{V}{RT} - \frac{1}{P} \right) dP \tag{13}$$

$$\ln \frac{f}{P} = Z - 1 - \ln(Z - B) - \frac{A}{2\sqrt{2}B} \ln \left(\frac{Z + 2.414B}{Z - 0.414B} \right) \tag{14}$$

The physical parameters of the three gases in Table 4 are brought into the written Matlab programmes to obtain the relationship between the fugacity coefficient and pressure of the three gases as shown in Fig. 4, which indicates that: the fugacity coefficient decreases gradually with the increase of the pressure at the same temperature; the higher the temperature, the larger the fugacity coefficient is at the same pressure. From 0 to 15 MPa, the fugacity coefficient of CH₄ decreases with the increase of pressure, and the higher the temperature, the smaller the fugacity coefficient, that is, the higher the temperature, the closer the fugacity is to the pressure, and the lower the temperature, the larger the difference between the fugacity and the pressure. CO₂ fugacity coefficient and the pressure of the relationship between the existence of sudden changes, 273.15 K, 283.15 K, 293.15 K fugacity coefficient curve gradient there is a sudden change, at this time the CO₂ is in the supercritical state of the transition from the gas state to the liquid state, at this time the fugacity coefficient decreased rapidly, the temperature of 303.15 K and 313.15 K, with the increase in the pressure of the fugacity coefficient of the sudden phenomenon disappeared. The fugacity coefficient of H₂O is significantly affected by pressure when H₂O is converted from gaseous state to liquid state under high pressure. When the temperature is 313.15 K, the pressure exceeds 2 MPa, the fugacity coefficient decreases abruptly and approaches zero, at which time H₂O is converted from a gas state to a liquid state. With the decrease of temperature, the critical temperature of phase transition gradually decreases. From 0 to 15 MPa, the fugacity coefficients decreased from 1.0 to 0.7 for CH₄, 1.0 to 0.2 for CO₂, and 1.0 to 0.0 for H₂O; the degree of variation of the fugacity coefficients of the three gases was inversely proportional to the critical temperature T_c and critical pressure P_c , and positively proportional to the excursion factor. For binary gas components¹⁵, the fugacity coefficients can be obtained by Eqs. (15) and (16).

$$\ln \varphi_i = \frac{b}{b_i}(Z - 1) - \ln(Z - B) - \frac{A}{B} \left(\frac{b}{b_i} - \frac{2 \sum y_j a_{ij}}{a} \right) \ln \frac{Z + B}{Z} \tag{15}$$

$$\ln \varphi_j = \frac{b}{b_j}(Z - 1) - \ln(Z - B) - \frac{A}{B} \left(\frac{b}{b_j} - \frac{2 \sum y_j a_{ij}}{a} \right) \ln \frac{Z + B}{Z} \tag{16}$$

$$a_i = \frac{0.45724R^2T_{ci}^2}{P_{ci}} \tag{17}$$

$$a_j = \frac{0.45724R^2T_{cj}^2}{P_{cj}} \tag{18}$$

$$b_i = \frac{0.07780RT_{ci}}{P_{ci}} \quad (19)$$

$$b_j = \frac{0.07780RT_{cj}}{P_{cj}} \quad (20)$$

$$a_{ij} = \sqrt{a_i a_j} (1 - k_{ij}) \quad (21)$$

In formula: T_{ci} , T_{cj} are the critical temperatures of single components i , j , respectively, K; P_{ci} , P_{cj} are the critical pressures of single components i , j , respectively, MPa; φ_i , φ_j are the fugacity coefficients of single components i , j , respectively.

For binary components, the coefficients a , b are calculated based on the van der Waals mixing rule using the following equation:

$$a = \sum_i \sum_j y_i y_j a_{ij} \quad (22)$$

$$b = \sum_i y_i b_i \quad (23)$$

The result of the fugacity expression is given by the following equation:

$$f_i = y_i \varphi_i p \quad (24)$$

In formula: f_i , f_j is the fugacity of single component i , j , MPa.

Interaction energy

The interaction energy is the work done by the interaction force between gas molecules and coal surface after they approach each other, representing the stability of the system. At the same time, the adsorption capacity of the adsorbate for the adsorbate can be measured. The interaction energy is defined as follows:

$$E_{\text{int}} = E_{\text{coal/gas}} - E_{\text{coal}} - E_{\text{gas}} \quad (25)$$

In the formula, $E_{\text{coal/gas}}$ is the total energy of coal after adsorption of gas molecules, kJ/mol; E_{coal} and E_{gas} are the energies of the coal and gas molecules, kJ/mol, respectively; E_{int} is the interaction energy, kJ/mol; A negative value of E_{int} is an exothermic reaction, and the larger its absolute value, the stronger the adsorption.

Adsorption model reliability validation

In order to verify the correctness of the constructed gas-fat coal molecule and adsorbent small molecule models as well as the correctness of the force field parameter settings, the adsorption isotherms of CH_4 and CO_2 molecules on the gas-fat coal macromolecule model were compared with the experimental data at the temperature of 293.15 K and the pressures of 0.01–15 MPa, using the gas-fat coal macromolecule model as the adsorbent. The experiment was carried out by using HCA-type high-pressure volumetric gas adsorption device for the adsorption of CH_4 and CO_2 single-component gases on gas-fat coal, which mainly consists of a vacuum drying system, a degassing system, an inflatable system, an adsorption system and a detection system. Put the gas fertilizer coal in the coal sample tank, open the constant temperature water bath device (60°C), check the airtightness connected to the vacuum pump, open the vacuum pump for degassing the system, vacuum to 4 Pa below and then continuously degassed for 20 min, put the coal sample tank in the constant temperature water bath, the temperature is set to 20°C , open the piston, calibrate the level of the level bottle with the level of liquid in the tube to the same level, open the high pressure valve in the coal sample tank, the CH_4 , CO_2 into the tank, when the adsorption rate of coal samples is less than $0.5\text{cm}^3/\text{h}$, when the adsorption reaches equilibrium. Calibrate the liquid level in the leveling bottle and measuring tube to the same level again. The difference between the initial and post adsorption equilibrium liquid level of the measuring tube is the adsorption amount.

As shown in Fig. 5, the trend of adsorption isotherms of different gases obtained from experiments and molecular simulation is basically the same, with a slight deviation in values, and the experimental data are smaller than the simulated data, which is due to the fact that in this paper, only the structure of organic macromolecules is taken into account in the process of constructing coal macromolecule model, and inorganic structures, such as quartz, silicon oxide, and silicate, are ignored, which results in the macromolecule model having slightly higher pore volumes and specific surface areas so that the simulated adsorption amount is slightly higher than the experimental value. The above proves the rationality of the gas-fat coal macromolecule and adsorbent small molecule models constructed in this paper as well as the force field parameter settings.

Results and discussion

Adsorption amount of CH_4 , CO_2 and H_2O

The adsorption isotherms of gas-fat coal macromolecule model for adsorption of CH_4 , CO_2 and H_2O molecules at different temperatures are shown in Fig. 6a–c. The absolute adsorption amounts of all three gases increase with the increase of equilibrium pressure, and the adsorption can be divided into three stages: rapidly adsorption, slowly adsorption, and gently adsorption stage. The adsorption amounts of gas-fat coal adsorption of CH_4 , CO_2 and H_2O molecules were fitted using the Langmuir model, and the curves conformed to the Langmuir I-type

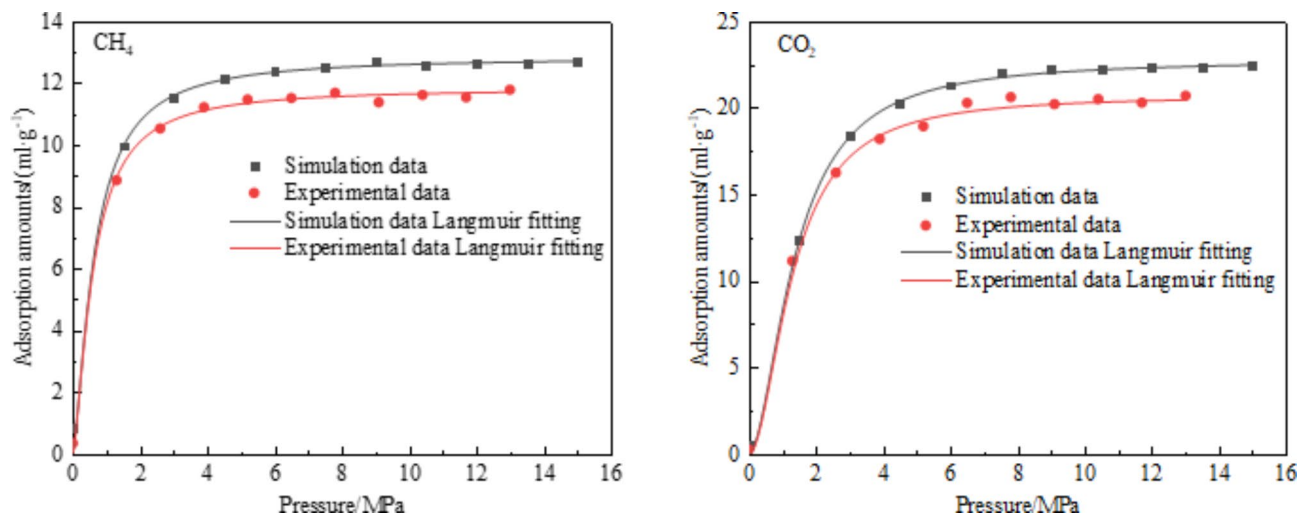


Fig. 5. Simulation of adsorption compared with experiment.

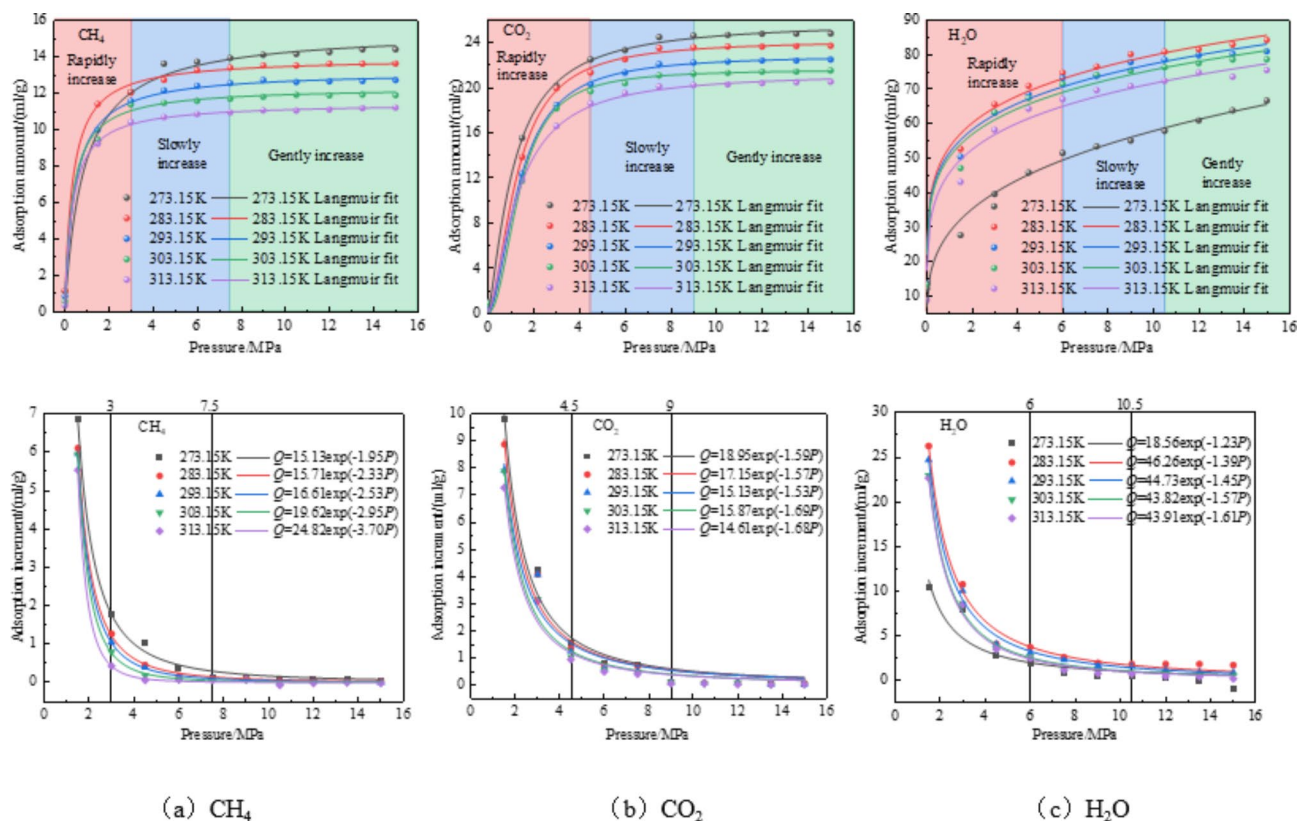


Fig. 6. Adsorption isotherm of gas-fat coal.

isotherms. The fitting results are shown in Table 5, and the R^2 are all greater than 0.99. The basic assumptions of the Langmuir model include: the existence of adsorption sites on the surface of the adsorbent and that adsorbent molecules can only be adsorbed to these sites in a monolayer. The adsorption sites are homogeneous in both the thermodynamic and kinetic senses. The surface of the adsorbent is homogeneous in properties. The molecules of adsorbent do not interact with each other, and the adsorption-desorption process is in dynamic equilibrium. Non-homogeneity in the number and spatial distribution of coal body pores. The pores of the coal body are characterized by multiple scales, diverse pore types, complex structure and strong anisotropy and non-homogeneity, but the internal surface properties of the pore structure have the characteristic of homogeneity. Although the pore structure of the coal body is nonhomogeneous, it still meets the Langmuir I-type isotherm.

System type	Temperature/K	a/(ml/g)	b/(1/MPa)	R ²
Gas fat coal and CH ₄ system	273.15	15.414	1.165	0.9884
	283.15	13.895	2.882	0.9924
	293.15	13.176	2.258	0.9958
	303.15	12.305	2.841	0.9852
	313.15	11.445	2.879	0.9996
Gas fat coal and CO ₂ system	273.15	25.825	1.783	0.9884
	283.15	24.161	1.752	0.9924
	293.15	22.833	1.928	0.9958
	303.15	21.563	1.817	0.9852
	313.15	21.274	1.714	0.9996
Gas fat coal and H ₂ O system	273.15	58.086	0.353	0.9927
	283.15	67.997	0.856	0.9983
	293.15	65.811	0.966	0.9925
	303.15	66.141	0.832	0.9964
	313.15	61.345	0.943	0.9914

Table 5. Langmuir constants of CH₄, CO₂ and H₂O gas adsorbed by gas-fat coal macromolecule model.

The amount of CH₄, CO₂ and H₂O molecules adsorbed at different temperatures increases with increasing equilibrium pressure, and the increase in equilibrium pressure promotes the contact of adsorbate molecules with the surface of the adsorbent matrix, which allows more adsorbate molecules to be retained in the adsorbed phase. The increase in equilibrium pressure has a significant promoting effect on the adsorption of single component gases, but there is a critical point in this promoting effect, when the pressure is below the critical equilibrium pressure, the adsorption amount rapidly increases with the increase of equilibrium pressure, while when the equilibrium pressure is greater than the critical pressure, the adsorption amount slowly increases. The critical equilibrium pressures for the three systems of gas-fat coal CH₄, gas-fat coal CO₂, and gas-fat coal H₂O are 3 MPa, 4.5 MPa, and 6 MPa, respectively. This is mainly because coal has a smaller adsorption amount for CH₄, while it has a larger adsorption amount for CO₂ and H₂O, making it difficult to achieve equilibrium, achieving equilibrium requires a greater equilibrium pressure. As can be seen from Fig. 6, the adsorption increment of CH₄, CO₂ and H₂O molecules with the increase of pressure showed an exponential decay trend of firstly decreasing rapidly, then slowly decreasing, and finally decreasing gently. At the same pressure, the lower the temperature the larger the adsorption increment, indicating that temperature plays a negative role in the adsorption of CH₄ and CO₂. According to the size of the adsorption increment, the adsorption process is divided into three phases of rapidly increase, slowly increase and gently increase in the adsorption process in this paper.

With the increase of temperature, the saturated adsorption amount of CH₄ and CO₂ by gas-fat coal gradually decreased, the saturated adsorption amount of CH₄ decreased from 14.37 ml/g at 273.15 K to 11.18 ml/g at 313.15 K, the saturated adsorption amount of CH₄ decreased by 22.20%; the adsorption rate of CH₄ molecules at 283.15 K was faster compared to that at 273.15 K, and the increase of temperature led to the increase of kinetic energy of CH₄ molecules, The increase of CH₄ molecules' kinetic energy increased the contact probability between CH₄ molecules and coal pore surface, which improved the adsorption rate, and the saturated adsorption amount of CO₂ decreased from 24.7 ml/g at 273.15 K to 20.4 ml/g at 313.15 K, which was a decrease of 17.4%. On the contrary, the saturated adsorption amount of H₂O was the lowest at 273.15 K, only 66.61 ml/g. The gas-fat coal macromolecules showed inhibition of water molecule adsorption at low temperature, which was caused by two reasons: on the one hand, the movement rate of molecules under low temperature was low, and it was difficult to reach adsorption equilibrium within a short period of time; On the other hand, the condensation of water vapor at low temperature changes part of the water from gaseous phase to liquid phase, which blocks the pores and forms water locks, thus inhibiting the adsorption. The adsorption of H₂O molecules increased from 66.61 ml/g to 84.21 ml/g when the temperature was increased from 273.15 K to 283.15 K. When the temperature was increased from 283.15 K to 313.15 K, the adsorption decreased to 75.46 ml/g, and the saturation adsorption decreased by 10.39%, and the adsorption of H₂O molecules in the coal was inhibited at both low and high temperature, which is in agreement with the results of Gao¹⁵ obtained. In gas-fat coal, according to the magnitude of decrease in gas adsorption at elevated temperatures, the adsorption of methane is most sensitive to temperature, and the temperature has less influence on the adsorption of CO₂ and H₂O molecules. The increase of temperature is not conducive to adsorption, higher temperature will make the adsorbate molecules obtain higher kinetic energy, so that the adsorbate molecules have high enough energy to overcome the bonding of van der Waals force, electrostatic force and hydrogen bonding force to change from adsorption to free state, and high temperature will inhibit the molecules from the free state to adsorption state, and also show that the adsorption of CH₄, CO₂ and H₂O molecules by the Jixi gas-fat coal is an exothermic reaction.

Under the same conditions of temperature and pressure, the adsorption of H₂O molecules by gas-fat coal was the largest, followed by CO₂, and CH₄ was the smallest, and the adsorption of the three adsorbates by gas-fat coal was in the following order from the hardest to the easiest: CH₄ < CO₂ < H₂O, which is in agreement with the conclusions obtained by^{17–22}. The reasons for the different saturation adsorption amounts of the three adsorbates are mainly related to their own physical properties. On the one hand, it is related to the molecular dynamics

radius of the three gases, the molecular dynamics radius from smallest to largest is: $\text{H}_2\text{O} < \text{CO}_2 < \text{CH}_4$, which is in the opposite order of the adsorption amount, mainly because the micropores used for the adsorption of H_2O are the most abundant, followed by CO_2 , and CH_4 molecules have the least space available for adsorption, and the smaller the pore size of the pore, the larger the potential of its adsorption.

The linear shape and smaller molecular dynamics diameter allow H_2O to enter smaller micropores, but due to the molecular sieve effect, CH_4 and CO_2 molecules cannot enter some micropores. The boiling point of CH_4 is lower than that of CO_2 and H_2O , which means that CH_4 is more likely to escape from the gas rich coal macromolecule structure through “evaporation”. CO_2 and H_2O have a permanent quadrupole moment, and the charge of CH_4 molecules is neutral. The quadrupole moment can enhance the electrostatic interaction between CO_2 and H_2O and coal molecules, making the molecule more easily “captured” by the coal pore surface. The adsorption of H_2O molecules in coal is mainly affected by the hydrogen bonding effect, which is greater than the van der Waals energy interactions. As the amount of adsorption increases, the strong hydrogen bonding between water molecules leads to capillary coalescence, and the coalescence of water gradually forms a new adsorption site, which results in a larger adsorption amount.

Potential energy distribution of CH_4 , CO_2 and H_2O

By analyzing the information on the energy distribution of adsorbate molecules during the adsorption of CH_4 , CO_2 and H_2O by gas-fat coal, the distribution of adsorption sites of different adsorbates can be obtained. Energy distribution represents the probability density of adsorbate molecules distributed in different energy regions, in other words, the potential energy distribution of adsorbate molecules in Jixi gas-fat coal, the region with the smallest interaction energy is the preferred adsorption site, the larger the absolute value of the potential energy at the adsorption site, the higher the adsorption potential well, the stronger the interaction with adsorbate, and the more likely to adsorb gas molecules, and the more preferred adsorption site. Comparison of the energy distribution at different temperatures can tell the effect of temperature on the migration of adsorption sites, and comparison of the potential energy curves at different pressures can tell the changes of adsorption sites during the adsorption of CH_4 , CO_2 , and H_2O on Jixi gas-fat coal¹⁶.

In this paper, the molecular scale adsorption sites as well as the potential energy probability density distributions were obtained, and the adsorption interaction energy distribution maps can determine the preferential adsorption sites on the surface of the coal molecules¹⁶, and the potential energy distribution curves of CH_4 , CO_2 , and H_2O molecules on a gas-fat coal macromolecule model at different temperatures are shown in Fig. 7. Define potential energy peaks as most significant interaction potentials. It is observed that the interaction energy probability distributions of CH_4 , CO_2 and H_2O molecules are poisson distributed, with their peaks corresponding to the potential energies of the most significant interaction sites, and the potential energy probability distributions are symmetrically distributed center on the most significant interaction potentials, and the peak heights of their probability distributions are in ascending order as $\text{CH}_4 > \text{CO}_2 > \text{H}_2\text{O}$, respectively. The energy range of CH_4 adsorption sites was $-32.81 \sim -7.85$ kJ/mol, CO_2 adsorption sites was $-15.32 \sim -53.84$ kJ/mol, and H_2O adsorption sites was $-18.65 \sim -100.73$ kJ/mol. The distribution curves of interaction energies during the adsorption of H_2O were wide and short, while the distribution curves of CH_4 adsorption were narrow and high. The distribution of H_2O adsorption sites was more dispersed and abundant, while the distribution of CH_4 adsorption sites was more concentrated but sparse, and the number of adsorption sites for CO_2 ranges between CH_4 and H_2O .

The peaks of the potential energy distribution curves are the most available interaction energies of CH_4 , CO_2 and H_2O molecules interacting with the macromolecule model of gas-fat coal during the adsorption process, and the larger the absolute value is, the stronger the interaction capacity is. In the adsorption process between gas-fat coal and the three adsorbates, H_2O has the largest most significant interaction potentials, and the most significant interaction potentials is located near -60 kJ/mol, which is the main adsorption site of H_2O molecules; CO_2 has the second largest most significant interaction potentials, and the peak is located at about -35 kJ/mol; and CH_4 has the smallest most significant interaction potentials, and the peak is located at about -23 kJ/mol.

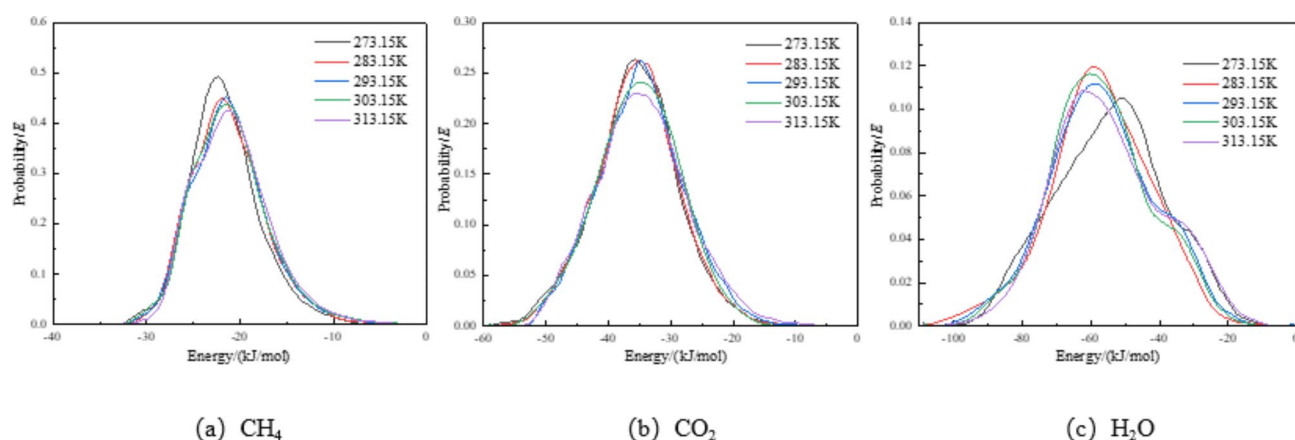


Fig. 7. Distribution of potential energy of single component adsorption at different temperatures.

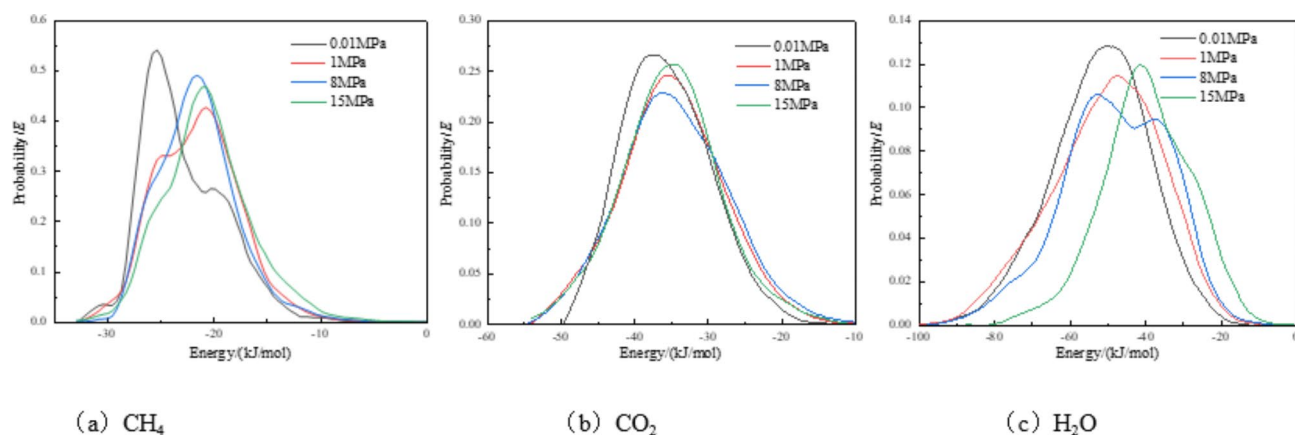


Fig. 8. Potential energy distribution of single component adsorption at different pressures at 293.15 K.

This indicates that the three gas molecules have different adsorption sites in the gas-fat coal macromolecule structure, and the absolute values of their interaction energies are from high to low: $\text{H}_2\text{O} > \text{CO}_2 > \text{CH}_4$, which is consistent with the order of adsorption amount of the three molecules.

Figure 7a shows the energy distribution of CH_4 when the temperature rises from 273.15 K to 313.15 K, the most significant interaction energy of CH_4 is shifted from -22.69 kJ/mol to -21.08 kJ/mol, and the peak value of the energy distribution curve gradually decreases, the increase in temperature leads to a gradual decrease in the adsorption potential corresponding to the most significant adsorption sites of CH_4 . The temperature increases to inhibit the adsorption of CH_4 molecules, the kinetic energy of CH_4 molecules increase, have more energy to break free from the adsorption site, to the free state conversion, to the low potential well adsorption site transfer. As the temperature increases, the peak value of the energy distribution curve of CH_4 gradually decreases, mainly because the increase in temperature leads to a decrease in the adsorption amount of the preferred adsorption site, resulting in a decrease in the probability density at that adsorption site. Figure 7 (b) shows the energy distribution diagram of CO_2 molecules, and the most significant interaction energy is less affected by temperature. As temperature increases, the peak value of the potential energy distribution decreases. Figure 7(c) shows the energy distribution of H_2O molecules, when the temperature is increased from 273.15 K to 293.15 K, the most significant interaction energy of H_2O molecules is shifted from -50.04 kJ/mol to -62.92 kJ/mol, which is moved to the adsorption site with higher adsorption potential well, and when the temperature is increased from 293.15 K to 313.15 K, the most significant interaction energy is shifted from -62.92 kJ/mol to -58.56 kJ/mol to the adsorption site with smaller interactions, indicating that the adsorption site of gas-fat coal adsorbed water molecules is susceptible to temperature, which is in agreement with the conclusions obtained by¹⁶, that both low and high temperatures play an inhibitory role in the adsorption of H_2O molecules.

The distribution of interaction energies during adsorption of single-component CH_4 , CO_2 and H_2O at different pressures at a temperature of 293.15 K is shown in Fig. 8, where four representative pressure points, 0.01 MPa, 1 MPa, 8 MPa and 15 MPa, were selected. It was found that the energy distribution curves of all three molecules, CH_4 , CO_2 and H_2O , shifted to the right with increasing pressure, and the adsorption sites shifted from the preferential adsorption sites with larger interaction energies to the secondary adsorption sites with smaller interaction energies. It was observed that the most significant interaction energy of CH_4 molecules migrated from -25.67 kJ/mol to -20.72 kJ/mol when the pressure was increased from 0.01 MPa to 1 MPa, and to -20.52 kJ/mol at 15 MPa; When the pressure is increased from 0.01 MPa to 1 MPa, the most significant interaction energy of CO_2 molecules migrates from -38.88 kJ/mol to -35.53 kJ/mol, and then to -33.64 kJ/mol at 15 MPa. When the pressure is increased from 0.01 MPa to 1 MPa, the most significant interaction energy of H_2O molecules migrates from -55.78 kJ/mol to -45.71 kJ/mol, and then to -41.53 kJ/mol at 15 MPa. This is because the adsorbate is preferentially adsorbed to the priority adsorption site with stronger interaction in the gas-fat coal macromolecule model, but the capacity of the priority adsorption site is limited, and when the priority adsorption site is occupied by the adsorbate molecules, the adsorbate molecules are transferred to the sub-priority adsorption site with the increase of the pressure, which causes the migration of the adsorption site, which is the most obvious with the equilibrium pressure increasing from 0.01 MPa to 1 MPa. When the equilibrium pressure was increased from 1 MPa to 15 MPa, the CH_4 molecules and CO_2 molecules moved to the right in smaller steps, while the H_2O molecules moved to the right in larger distances, which was mainly due to the fact that the primary adsorption sites had been filled and the second adsorption sites appeared in the adsorption process.

Probability density distributions for CH_4 , CO_2 and H_2O

The probability density distribution is the probability of adsorbate molecules appearing in each adsorption site, which can directly observe the distribution of adsorption sites of each adsorbate molecule in the macromolecule model of Jixi gas-fat coal, and the adsorption probability density distribution graphs can be used to analyze the whole process of the adsorption sites being filled. The probability density distributions of the molecular

adsorbates of CH_4 , CO_2 , and H_2O in the case of temperature of 293.15 K, pressure of 0.01 MPa, 1 MPa, 8 MPa, 15 MPa are shown in Fig. 9.

The first to occupy in the low-pressure adsorption stage is the preferential adsorption site, and the adsorption site with the largest probability density is the most available adsorption site. The probability density of single-component CH_4 adsorption process is shown in Fig. 9, at 0.01 MPa, CH_4 molecules adsorbed sporadically in the pores of the coal, the adsorption sites of CH_4 are very few and the density is very small, at this time it is a low-pressure adsorption stage. When the pressure was increased to 1 MPa, some CH_4 molecules were aggregated at the preferential adsorption sites, and most of the pore probability densities were blue, with only a small portion of the pore centers showing sporadic red color; The pressure was increased to 8 MPa, more and more CH_4 molecules were filled on the preferential adsorption sites, the density continued to increase, some of the preferential adsorption sites were filled, and the rest of the CH_4 molecules were shifted to the sub-preferential adsorption sites. As the pressure rises to 15 MPa, most of the pore center probability densities appear red, at which point a large number of preferential adsorption sites become saturated. Observing the probability density distribution, it can be seen that the probability density at the center of the pore is red, and the surrounding area is blue, and the adsorbate molecules firstly gather in large quantities at the center of the adsorption site, and then transfer to the surrounding area of the adsorption site. In the low-pressure adsorption stage, the adsorbate molecules firstly occupy the priority adsorption site, with the increase of adsorption amount, the priority adsorption site is saturated and the adsorbate molecules gradually transfer to the second priority adsorption site until the adsorption equilibrium is reached. The probability density distribution of the adsorption of CO_2 in the process of adsorption is shown in Fig. 9, and the law of adsorption of CH_4 applies to the adsorption of CO_2 molecules.

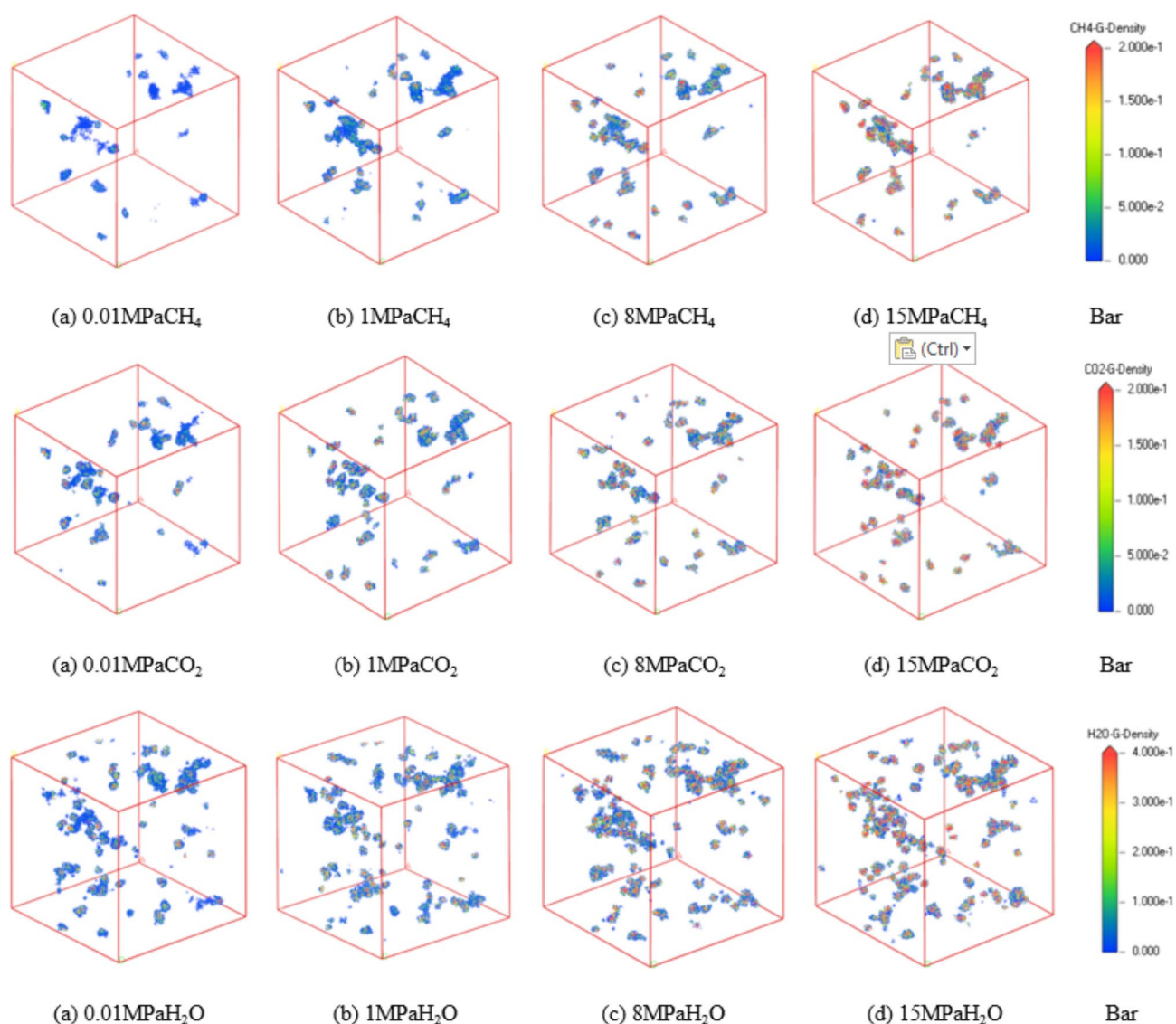


Fig. 9. Probability density distribution in CH_4 , CO_2 and H_2O adsorption process.

The probability density distribution of H₂O molecules under different pressures is shown in Fig. 9. When the pressure is 0.01 MPa, the adsorption sites in gas-fat coal are occupied by H₂O molecules, and the probability of most adsorption sites is small, mostly appearing blue. When the pressure rises to 1 MPa, H₂O molecules continue to fill the adsorption sites, and some probability density centers turn red. When the pressure rises to 8 MPa, some adsorption sites exhibit H₂O molecule aggregation, and the probability density at each adsorption site increases, gradually forming water clusters. New adsorption sites gradually form on the water clusters, leading to an increase in the number of adsorption sites. When the pressure rises to 15 MPa, the probability density appears red, and the adsorption sites tend to become saturated.

According to the distribution of gases in the gas-fat coal macromolecule model, it can be seen that the probability density located around the model is larger than that in the center of the model, indicating that most of the adsorption sites are located in the surrounding area of the model, and there are fewer sites located in the center of the model, and most of the adsorbates are adsorbed at the boundaries of the model.

Comparing the probability densities of the adsorption processes of CH₄, CO₂ and H₂O, it can be seen that the adsorption sites of H₂O molecules are the most abundant, followed by CO₂, and CH₄ molecules have the least adsorption sites. On the one hand, it is related to the molecular dynamics radius of the three adsorbates, the smaller the molecular radius is, the larger the adsorption space can be provided by the micropores inside the coal; On the other hand, it is related to the nature of the adsorbate itself, the H₂O molecules form new adsorption sites due to the capillary cohesion effect during the adsorption process, which results in the largest adsorption amount of the H₂O molecules.

Diffusion patterns of CH₄, CO₂ and H₂O

Molecular dynamics calculations of gas diffusion using the Focite module in MS can be used to obtain the Mean-Square Displacement(MSD) curves of different gases in the coal macromolecular structure, where the Mean-Square Displacement (MSD) is: the diffusion coefficient is the rate of change of the particle's MSD with time, which is obtained from Einstein's formula (26)²³.

$$D = \lim_{t \rightarrow \infty} \frac{1}{6N_a t} \left\langle \sum_{i=1}^N [r_i(t) - r_i(0)] \right\rangle^2 \quad (26)$$

In formula: D is the gas diffusion coefficient, m²/s; $r_i(t)$, $r_i(0)$ are the position of particle i at moment t and the initial moment; t is the simulation time, ps; N_a is the number of particles.

The mean square displacement of CH₄, CO₂, and H₂O molecules in the macromolecular structure of gas-fat coal at different temperatures and pressures of 15 MPa over time is shown in Fig. 10. The diffusion coefficient results calculated by the Einstein equation are shown in Table 6. As shown in the figure, the mean square displacement slopes of CH₄, CO₂, and H₂O gas molecules gradually increase with increasing temperature, and the diffusion coefficient of the gas is directly proportional to temperature.

From Table 6, it can be seen that the temperature increased from 273.15 K to 313.15 K, and the diffusion coefficient of CH₄ molecules increased from 0.42×10^{-9} m²/s to 0.82×10^{-9} m²/s, with a diffusion coefficient of CO₂ molecules ranging from 1.02×10^{-9} m²/s to 1.21×10^{-9} m²/s, with a diffusion coefficient of H₂O molecules ranging from 1.13×10^{-9} m²/s to 1.82×10^{-9} m²/s. This is similar to the results obtained by²⁴, the diffusion coefficients of the three gases at the same temperature have the relationship of H₂O > CO₂ > CH₄, which is consistent with the inverse order of the dynamic radius of the three molecules, the smaller the radius of the gas molecules, the more easily to enter into the coal micropore, the coal molecular wall has much less influence on its diffusion in the pore space, the more space it can move, and the larger diffusion coefficient. The diffusion coefficients of CO₂ and H₂O diffusion coefficients are greater than CH₄, indicating that injecting CO₂ and H₂O into the coal seam can replace CH₄ in the coal micropores. The diffusion coefficients of the three gas molecules in the coal macromolecule model are proportional to the temperature. The higher the temperature, the greater

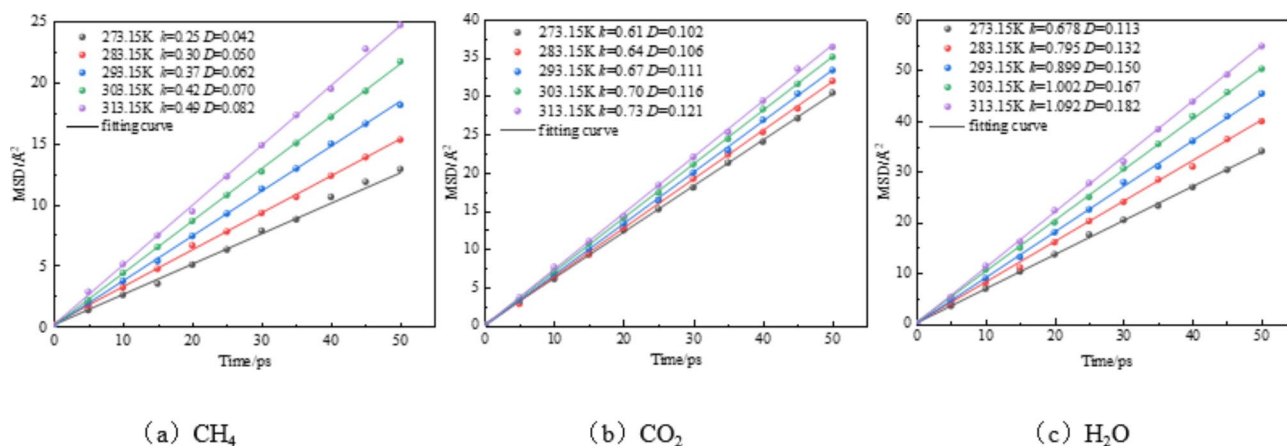


Fig. 10. Mean square displacement of CH₄, CO₂, and H₂O gases at different temperatures.

Temperature/K	Diffusion coefficient/ $1 \times 10^{-9} \text{m}^2 \cdot \text{s}^{-1}$		
	CH ₄	CO ₂	H ₂ O
273.15	0.42	1.02	1.13
283.15	0.50	1.06	1.32
293.15	0.62	1.11	1.50
303.15	0.70	1.16	1.67
313.15	0.82	1.21	1.82

Table 6. Diffusion coefficients of CH₄, CO₂ and H₂O at different temperatures.

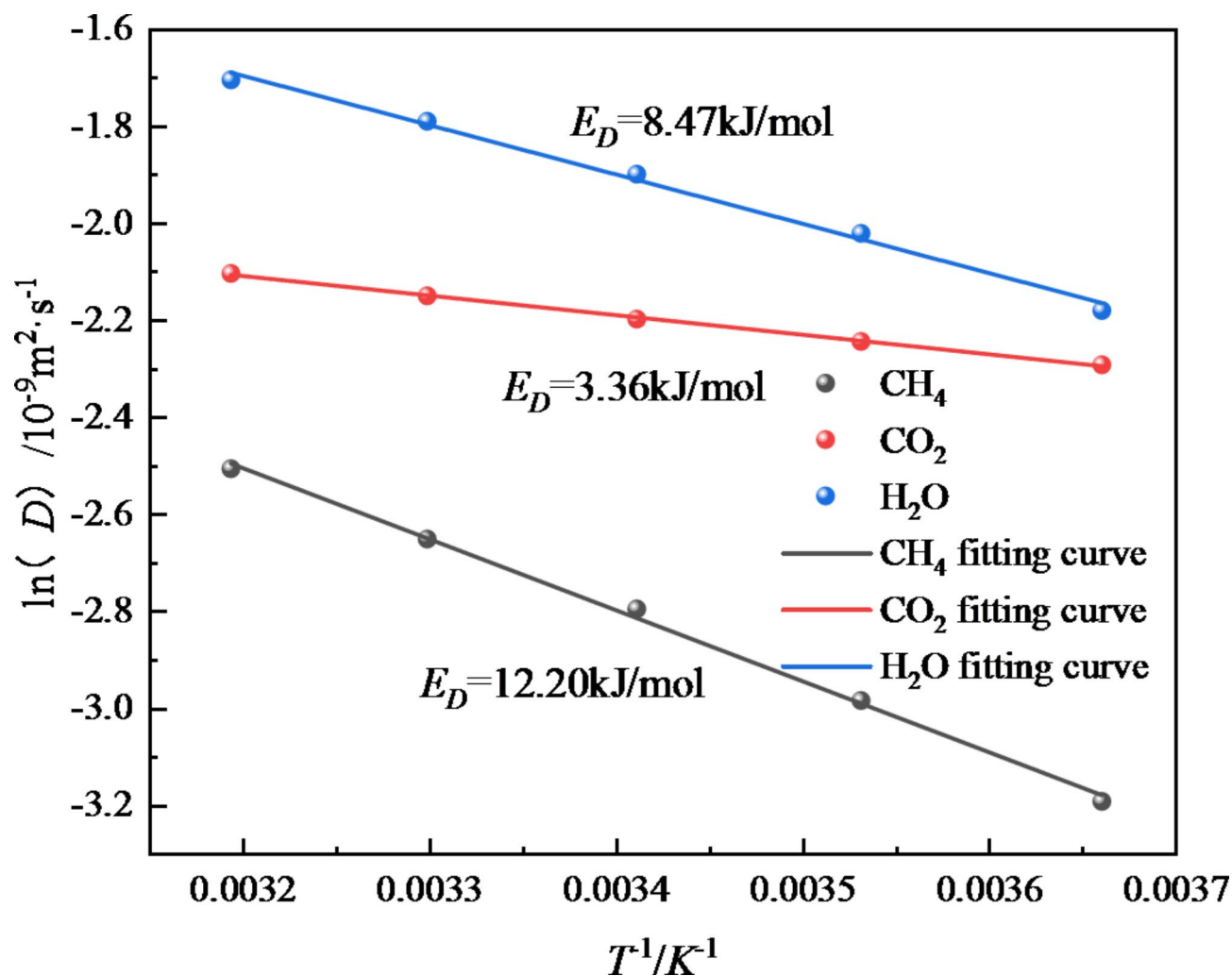


Fig. 11. Fitting curve between $\ln D$ and T^{-1} for CH₄, CO₂ and H₂O gases.

the internal energy of the molecules, and according to the theorem of conservation of energy, the internal energy will be converted into kinetic energy, which makes the molecules move faster and the easier it is to diffuse. High temperature reduces the viscosity of gas molecules, so that the diffusion resistance becomes smaller, high temperature will cause the expansion of the coal matrix structure, resulting in the opening of the originally closed pore orifices, increasing the connectivity of the fissures, making the effective gas diffusion channels in the coal body increase, and high temperature can promote the diffusion of the gas in the coal.

The diffusion coefficient indicates the speed of diffusion of adsorbate molecules, and the diffusion activation energy indicates the difficulty of adsorbate diffusion. The nature of the diffusion of various types of adsorbates in the coal body is the diffusion activation process²⁵, gas molecules from a certain equilibrium position to jump the potential barrier ΔG to reach another equilibrium position, the gas will diffuse, the diffusion process

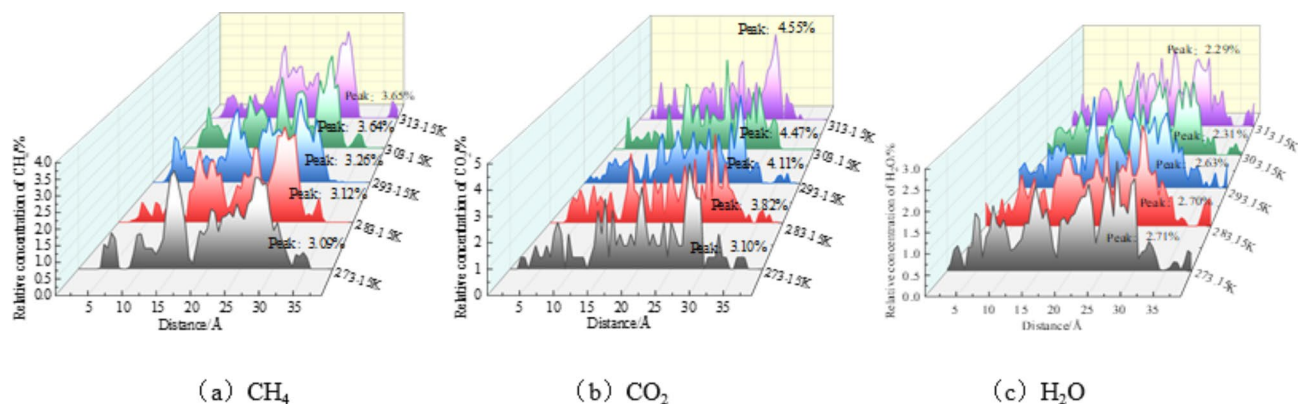


Fig. 12. Relative concentration distribution of CH₄, CO₂ and H₂O along the Z-axis at different temperatures.

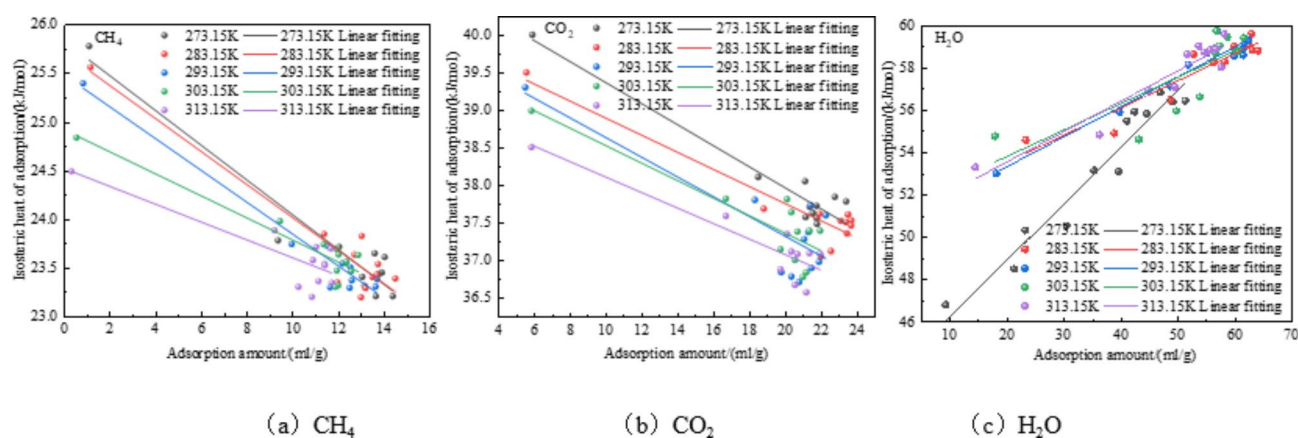


Fig. 13. Relationship between adsorption amount and isosteric heat of adsorption for CH₄, CO₂ and H₂O at different temperatures.

to overcome the potential barrier is called the activation energy of diffusion E_D , the activation energy of gas diffusion is commonly used in the Arrhenius formula²⁶ for the calculation, as shown in Eq. (27).

$$D = D_0 e^{-\frac{E_D}{RT}} \quad (27)$$

In formula: D_0 is the finger front factor, m^2/s ; E_D is the diffusion activation energy, kJ/mol , and R is the ideal gas constant, taken as $8.314 J/(mol \cdot K)$.

As shown in Fig. 11, the diffusion activation energies of CH₄, CO₂, and H₂O are 12.20 kJ/mol , 3.36 kJ/mol , and 8.47 kJ/mol , respectively, which are similar to the results calculated by [106]. The activation energies of diffusion from high to low are CH₄ > H₂O > CO₂. The activation energies of diffusion reflect the sensitivity of diffusive motion to temperature, and the diffusion of CO₂ is the most sensitive to temperature. It shows that within the coal macromolecules, CO₂ is more likely to diffuse, linear and discoidal molecules are affected by a larger effect than spherical molecules of the same volume equivalent, CO₂ is a linear molecule, CH₄ is a tetrahedron molecule, H₂O is a folded triatomic molecule, and the coal molecular wall has a much smaller effect on the diffusion of CO₂ in the pore space, resulting in smaller diffusion activation energy. CO₂ is more likely to diffuse phenomena, providing theoretical support for CO₂-ECBM technology.

Relative concentration distributions of CH₄, CO₂ and H₂O

To further study the distribution of CH₄, CO₂ and H₂O in gas-fat coal, the distribution of adsorbate molecules in gas-fat coal macromolecules can be obtained by analyzing the relative concentration along the Z-axis of different models after kinetic optimization from a microscopic point of view. The data in the figure are the average relative concentrations of CH₄, CO₂ and H₂O along the Z-axis at different temperatures. As can be seen in Fig. 12, the average relative concentration of CH₄ molecules in coal macromolecules shows a bimodal or trimodal distribution, with most CH₄ molecules in the middle part of the model showing a laminar distribution along the Z-axis; most of the CO₂ molecules are located in the range of 15~30 Å, with a band-like distribution along the direction of the Z-axis; and the distribution of the concentration of H₂O molecules show a multi-peak structure in the concentration distribution along the Z-axis direction, and they are distributed in multiple

clusters along the Z-axis direction. With the increase of temperature, the relative concentration peaks of CH₄ and CO₂ molecules gradually increased, while the relative concentration peaks of H₂O molecules gradually decreased.

Isosteric heat of adsorption of CH₄, CO₂ and H₂O

Isosteric heat of adsorption is an important parameter to characterize the adsorption behavior of coal, which can show the change rule of heat in the system, and it is often used to judge the physicochemical nature of coal adsorption, which is of great significance to reveal the adsorption law. Adsorbate molecules from the high energy level state into a low energy level state, there will be heat generation, this part of the heat generated is called heat of adsorption, adsorption heat of the nature of the adsorbate free state and adsorption state of the potential energy difference, to a certain extent, the heat of adsorption can reflect the adsorption capacity of the material²⁵. Adsorption of a certain amount, and then adsorbed a trace amount of adsorbate heat released is called the isosteric heat of adsorption [109], the isosteric heat of adsorption is calculated using the Clausius-Clapeyron²⁷ equation, as shown in Eqs. (28) and (29).

$$Q_{st} = RT^2 \left(\frac{\partial \ln P}{\partial T} \right)_q \quad (28)$$

$$\ln P = -\frac{Q_{st}}{RT} + C \quad (29)$$

In formula: Q_{st} is the isosteric adsorption heat, kJ/mol; T is the temperature, K; P is the pressure, MPa; R is the gas constant, 8.314 J/(mol·K). The equivalent adsorption lines for CH₄, CO₂ and H₂O were plotted according to $\ln P$ versus $1/T$ corresponding to different adsorption amounts, and the isosteric adsorption heat corresponding to different adsorption amounts was obtained by calculating the slopes.

The relationship between the amount of adsorption and the isosteric heat of adsorption of CH₄, CO₂ and H₂O at different temperatures is shown in Fig. 13. If the adsorbent material is homogeneous, the magnitude of the isosteric heat of adsorption is independent of the amount of adsorption, and when the surface of the adsorbent material has a non-homogeneous characteristic, the isosteric heat of adsorption varies with the amount of adsorption²⁸. The isosteric heat of adsorption of CH₄ and CO₂ decreases gradually with the increase of adsorption, in contrast the isosteric heat of adsorption of H₂O molecules increases gradually with the increase of adsorption, which suggests that the distribution of pores inside the coal body is not homogeneous. The variation of the isosteric heat of adsorption is affected on the one hand by the non-homogeneity of the coal body, which has an anisotropic pore distribution, which leads to the decrease of the isosteric heat of adsorption with the increase of adsorption amount. The pores have different adsorption potentials at each position, and the adsorbate molecules preferentially occupy the adsorption sites in the high adsorption potential wells, when the isosteric heat of adsorption is released to the greatest extent; The number of high-potential energy adsorption sites is limited, and when the high-energy adsorption sites are saturated, each adsorbate gradually transfers to the second-priority adsorption sites, and the interaction energy between the adsorbate and the coal decreases, leading to a decrease in the isosteric heat of adsorption. On the other hand, influenced by the interactions between adsorbates, the interactions between adsorbates gradually increase, resulting in a gradual increase in the isosteric heat of adsorption. Within the adsorption system of Jixi gas-fat coal, these two interactions have opposite effects on the isosteric heat of adsorption. CH₄ and CO₂ molecules dominate the non-homogeneous interactions of the coal body during the adsorption process, so the heat of adsorption gradually decreases, while H₂O molecules gradually dominate the H₂O-H₂O interactions during adsorption, which results in the heat of adsorption increasing gradually with the increase of adsorption amount. The ranges of isosteric heat of adsorption of CH₄, CO₂ and H₂O are 23.21 ~ 25.72 kJ/mol, 36.52 ~ 39.95 kJ/mol and 46.45 ~ 58.74 kJ/mol, respectively, which are similar to the results obtained from the calculations of Zheng Zhong²⁰, and the isosteric heat of adsorption of CH₄ and CO₂ are both less than 42 kJ/mol, so the adsorption of the two gases on the coal body is physical adsorption, while the isosteric heat of adsorption of H₂O molecules is greater than 42 kJ/mol, which is beyond the scope of physical adsorption. The isosteric heat of adsorption of H₂O is the largest, the isosteric heat of adsorption of CO₂ is the second, and the isosteric heat of adsorption of CH₄ is the smallest, which is consistent with the order of the adsorption amount of the three adsorbate. The isosteric heat of adsorption of CH₄ and CO₂ decreases rapidly in the low-pressure stage, and then decreases slowly with the increase of the pressure; the isosteric heat of adsorption of the H₂O molecule increases rapidly in the low-pressure stage, and then the isosteric heat of adsorption increases slowly when the pressure reaches a certain point.

The adsorption of CH₄, CO₂ and H₂O molecules on Jixi gas-fat coal is a dynamic equilibrium process of adsorption and desorption, the adsorption process is an exothermic reaction, and the desorption process is an adsorptive reaction, with the increase of adsorption amount, the adsorption sites gradually saturated, and the adsorption behaviors were gradually weakened, resulting in a decrease in the isosteric heat of adsorption.

The isosteric adsorption heat at different adsorption amounts at temperatures ranging from 273.15 to 313.15 K was calculated using Material Studio software. The Clausius-Clapeyron equation is used in MS software to calculate isosteric adsorption heat. Isosteric adsorption heat of CH₄, CO₂ and H₂O at different temperatures and adsorption amount are shown in Tables 7, 8, 9 and 10. The mean isosteric adsorption heat at different temperatures is calculated by taking the average of the isosteric adsorption heat at different adsorption amount at different temperatures.

With the increase of temperature, the isosteric heat of adsorption of CH₄ and CO₂ slightly decreased, and the increase in temperature was not conducive to the adsorption behavior, and the isosteric heat of adsorption of H₂O firstly increased and then decreased, which was consistent with the change of adsorption amount.

TEM/K	273.15		283.15		293.15		303.15		313.15	
Data point	ADS amount	ISO heat	ADS amount	ISO heat	ADS amount	ISO heat	ADS amount	ISO heat	ADS amount	ISO heat
1	1.12	25.78	1.18	25.56	0.86	25.40	0.35	24.50	0.57	24.54
2	9.37	23.79	11.38	23.85	9.97	23.75	9.22	23.89	9.45	23.68
3	12.04	23.72	13.02	23.83	11.54	23.73	11.03	23.72	11.36	23.45
4	13.59	23.65	12.70	23.64	12.33	23.56	11.68	23.70	11.95	23.59
5	14.02	23.62	13.73	23.54	12.18	23.55	10.89	23.58	12.01	23.34
6	13.90	23.46	13.67	23.43	12.53	23.51	11.40	23.54	12.87	23.54
7	13.76	23.44	13.50	23.41	13.69	23.39	11.41	23.53	12.36	23.37
8	13.05	23.41	14.49	23.40	12.59	23.38	11.13	23.37	11.94	23.28
9	13.14	23.32	11.96	23.36	13.63	23.31	11.71	23.35	12.56	23.37
10	14.38	23.22	13.19	23.30	11.65	23.31	10.26	23.31	11.99	23.22
11	13.63	23.21	12.99	23.20	12.50	23.30	10.85	23.21	11.87	23.21
Mean/kJ.mol ⁻¹	23.69		23.68		23.65		23.61		23.53	

Table 7. Isotheric adsorption heat of CH₄ at different temperatures and adsorption amount. *TEM* temperature, *ADS amount* adsorption amount/ mL/g, *ISO heat* isotheric heat/kJ/mol.

TEM/K	273.15		283.15		293.15		303.15		313.15	
Data point	ADS amount	ISO heat	ADS amount	ISO heat	ADS amount	ISO heat	ADS amount	ISO heat	ADS amount	ISO heat
1	5.93	39.83	5.60	39.37	5.53	39.38	5.88	38.96	5.88	38.58
2	18.50	37.95	18.81	37.56	18.32	37.89	16.70	37.80	16.70	37.67
3	21.11	37.90	21.92	37.49	21.42	37.82	20.11	37.79	20.11	37.43
4	22.77	37.69	23.51	37.49	22.27	37.69	20.35	37.62	20.35	37.20
5	23.40	37.63	23.69	37.41	21.31	37.47	21.36	37.37	21.36	37.18
6	21.76	37.57	23.10	37.41	21.06	37.37	21.96	37.37	21.96	37.17
7	21.39	37.56	23.40	37.38	21.89	37.07	20.69	37.36	20.69	37.17
8	21.55	37.48	23.68	37.34	21.47	36.99	19.75	37.13	19.75	36.96
9	21.15	37.42	23.44	37.24	19.79	36.94	20.55	36.99	20.55	36.76
10	21.77	37.41	22.56	37.00	20.35	36.88	21.19	36.82	21.19	36.66
11	21.78	37.33	21.99	36.93	20.78	36.80	21.00	36.76	22.34	37.28
Mean/kJ.mol ⁻¹	37.80		37.51		37.48		37.45		37.28	

Table 8. Isotheric adsorption heat of CO₂ at different temperatures and adsorption amount. *TEM* temperature, *ADS amount* adsorption amount/ mL/g, *ISO heat* isotheric heat/kJ/mol.

TEM/K	273.15		283.15		293.15		303.15		313.15	
Data point	ADS amount	ISO heat	ADS amount	ISO heat	ADS amount	ISO heat	ADS amount	ISO heat	ADS amount	ISO heat
1	57.92	46.81	23.25	54.64	18.10	52.96	17.85	54.77	14.41	53.30
2	21.21	48.52	38.74	54.97	39.68	55.85	43.08	54.62	36.17	54.84
3	30.36	50.56	48.63	56.54	48.58	57.08	49.67	55.96	44.70	56.94
4	35.18	53.16	52.67	58.69	51.77	58.08	53.78	56.62	49.41	57.10
5	39.55	53.11	56.30	58.32	54.92	58.63	56.69	58.95	51.56	58.64
6	41.00	55.50	58.10	58.34	56.78	59.70	56.48	58.71	53.55	59.02
7	42.30	55.93	59.84	59.06	59.86	58.50	57.25	59.02	54.46	58.74
8	44.49	55.83	62.39	59.10	61.37	58.54	56.69	59.75	55.64	58.85
9	46.83	56.84	63.01	58.89	61.35	58.81	58.61	59.45	57.53	58.02
10	49.04	56.39	62.87	59.66	61.64	59.12	60.42	58.79	56.57	58.88
11	51.24	56.45	64.01	58.86	62.25	59.23	61.47	59.41	58.05	59.58
Mean/kJ.mol ⁻¹	53.56		57.92		57.86		57.82		57.63	

Table 9. Isotheric adsorption heat of H₂O at different temperatures and adsorption amount. *TEM* temperature, *ADS amount* adsorption amount/ mL/g, *ISO heat* isotheric heat/kJ/mol.

Pressure/MPa	Interaction energy of CH ₄ /kJ·mol ⁻¹				
	273.15 K	283.15 K	293.15 K	303.15 K	313.15 K
0.01	-180.778	-142.777	-121.499	-114.344	-90.1083
1	-664.196	-644.402	-555.727	-515.832	-517.486
8	-805.875	-789.661	-789.858	-745.102	-685.013
15	-929.187	-844.418	-830.159	-826.752	-818.059

Table 10. Total interaction energy of CH₄.

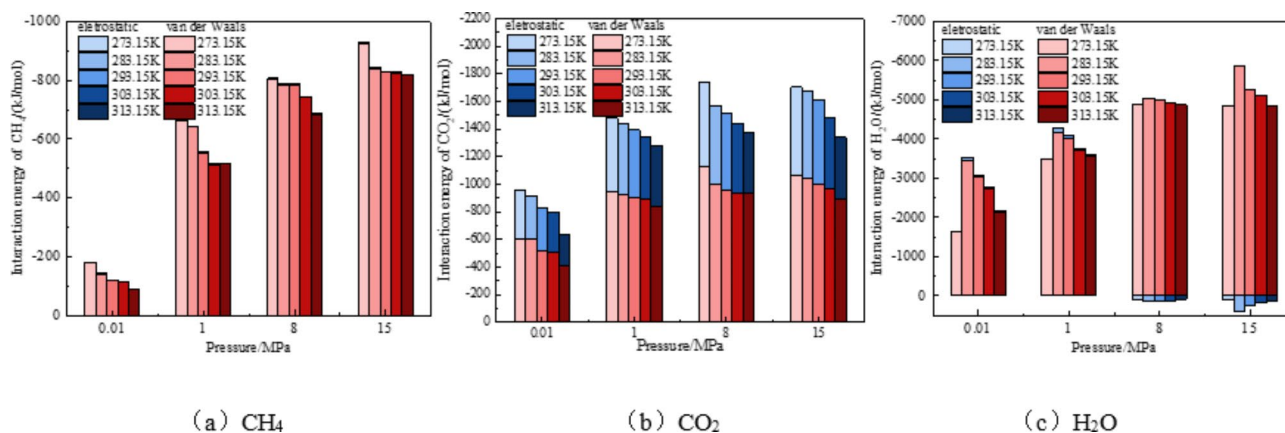


Fig. 14. Interaction energy of single component CH₄, CO₂ and H₂O adsorption at different temperatures.

Pressure/MPa	Interaction energy of CO ₂ /kJ·mol ⁻¹				
	273.15 K	283.15 K	293.15 K	303.15 K	313.15 K
0.01	-956.131	-919.924	-827.9	-801.807	-632.603
1	-1480.77	-1441.03	-1392.33	-1348.95	-1281.09
8	-1735.64	-1571.16	-1519.23	-1442.63	-1379.44
15	-1705.38	-1679.37	-1609.7	-1483.36	-1340.12

Table 11. Total interaction energy of CO₂.

It is observed that for CH₄ and CO₂, which are adsorbed in larger quantities, the isosteric adsorption heat data points become scattered in the high adsorption amount stage. The Monte Carlo method is a numerical computational method centered on probabilistic statistical theory. The simulation process begins with the development of an appropriate stochastic process or probabilistic model for a given problem so that the mathematical expectation of the probabilistic event is equal to the solution to the problem. There will be random rise and fall of adsorbate molecules within the system of this method, the number of adsorbate molecules is not a conserved quantity, and the adsorption process is an open system for adsorbate molecules in the pores of the adsorbent, and the adsorbate molecules within the pores can exchange substances and energy. With the increase of adsorption amount, the high potential energy adsorption sites are gradually occupied, and the adsorbate is gradually shifted to the sub-priority adsorption sites. When the adsorption amount reaches a certain level, the adsorbate molecules gradually tend to saturation, and the insertion and deletion of adsorbate particles become frequent at that stage, which is in the process of dynamic equilibrium, which leads to the phenomenon of random rise and fall of the isosteric heat of adsorption of CH₄ and CO₂ at high adsorption amount, resulting in the dispersion of the data of the isosteric heat of adsorption, which is permissible.

Interaction energy of CH₄, CO₂ and H₂O

The interaction energy represents the intensity of the interaction between gas and coal during the adsorption process, which to some extent reflects the stability of the gas adsorption state. The interaction during the adsorption process is the sum of the interaction energy between adsorbent-adsorbate and adsorbate-adsorbate. There are mainly three types of interactions between coal molecules and gas molecules: van der Waals force, electrostatic force, and hydrogen bonding force²⁹. To further investigate the relationship between adsorption capacity, adsorption heat, and interaction energy, the interaction energy during the adsorption process of single component CH₄, CO₂, and H₂O was studied. The interaction energy of single component CH₄, CO₂, and H₂O

Pressure/MPa	Interaction energy of H ₂ O /kJ·mol ⁻¹				
	273.15 K	283.15 K	293.15 K	303.15 K	313.15 K
0.01	-1643.69	-3537.15	-3070.58	-2752.94	-2158.86
1	-3489.74	-4268.64	-4097.77	-3762.14	-3593.72
8	-4787.16	-4954.95	-4905.67	-4862.53	-4862.53
15	-4741.05	-5773.86	-5483.03	-4861.34	-4985.70

Table 12. Total interaction energy of H₂O.

adsorbed in the Jixi gas fertilizer coal macromolecular model at five temperatures (273.15 K, 283.15 K, 293.15 K, 303.15 K, 313.15 K) and four pressures (0.01 MPa, 1 MPa, 8 MPa, 15 MPa). is shown in Fig. 14.

The interaction energy gradually increases with the increase of pressure, and decreases with the increase of temperature. The total interaction energies of CH₄, CO₂, and H₂O molecules under different temperature and pressure conditions are shown in Tables 10, 11 and 12. The maximum absolute value of the adsorption interaction energy of H₂O molecules is -1643.69 kJ/mol~5773.86 kJ/mol, The interaction energy of CO₂ takes the second place, ranging from -956.131 kJ/mol to -1705.38 kJ/mol, The minimum interaction energy of CH₄ is -180.778 kJ/mol~-929.187 kJ/mol, and the calculated results are similar to^{8,16,24,30}. During the adsorption process of H₂O molecules, the interaction energy is the highest, followed by the interaction energy of CO₂, and the interaction energy of CH₄ is the lowest, which is consistent with the order of adsorption capacity of the three adsorbents. As the temperature increases, the interaction energy decreases, which is consistent with the trend of adsorption capacity changing with temperature. Gas molecules are adsorbed into the pores of coal through interactions, and the adsorption amount is positively correlated with the interaction energy.

The interaction energy between CH₄ and CO₂ during adsorption is mainly composed of van der Waals forces and electrostatic forces. CH₄ and CO₂ are polar molecules with charged atoms. When two polar molecules approach each other, they undergo the phenomenon of homopolar repulsion and heteropolar attraction. The attraction effect caused by the orientation of these polar molecules is called orientation effect, also known as electrostatic force, which is related to the dipole moment and quadrupole moment of polar molecules, and the larger the dipole moment, the stronger the orientation effect. More than 99% of the interaction energy in the CH₄ adsorption process was van der Waals energy, and van der Waals interaction energy dominated the CH₄ adsorption process. The interaction energy in the CO₂ adsorption process was dominated by van der Waals interactions, which accounted for 64.41%, and the rest were electrostatic interactions, which accounted for 35.59%. Due to the existence of quadrupole moments, CO₂ adsorption has a large electrostatic interaction, while CH₄ does not exist dipole and quadrupole moments, so the electrostatic interaction between CH₄ molecules and coal molecules is weak, but there is a certain polarisation rate, and in the process of adsorption, the van der Waals force is mainly derived from dispersive and induced forces. During the adsorption of CO₂, the van der Waals force mainly comes from the directional force caused by the inherent dipole reversal. The interaction energy in the adsorption process of H₂O molecules is mainly dominated by hydrogen bonding, accounting for about 98% of the total interaction energy, supplemented by van der Waals interactions, accounting for 2%. On the one hand, the water molecules form stable hydrogen bonding structure with the polar functional groups on the coal surface, on the other hand, with the adsorption, the water molecules undergo capillary condensation phenomenon and form water clusters, and hydrogen bonding is generated between H₂O-H₂O. With the increase of pressure, when the pressure increases to 8 MPa, the van der Waals energy becomes positive, and the H₂O molecules adsorbed in the early stage are repelled from those adsorbed in the later stage, and the van der Waals energy becomes a negative energy term in the adsorption process of H₂O. The hydrogen bonding energy is always negative, which is a positive energy term in the adsorption process of H₂O molecules, and it is continuously enhanced with the increase of pressure. The absolute value of the hydrogen bonding energy is greater than the absolute value of the van der Waals interaction energy, and the overall interaction energy is negative and adsorption can still occur. When the pressure is 15 MPa, the interaction energy of H₂O molecules is 3.46 times that of CO₂ molecules and 6.37 times that of CH₄ molecules.

Conclusion

- (1) The adsorption amount of CH₄, CO₂, and H₂O increases with the increase of pressure, and the adsorption isotherms are consistent with Langmuir I isotherms. With the increase in temperature, the saturated adsorbed amount of CH₄ decreased from 14.37 ml/g at 273.15 K to 11.18 ml/g at 313.15 K, which is a decrease of 22.20%, and the saturated adsorbed amount of CO₂ decreased from 24.7 ml/g at 273.15 K to 20.4 ml/g at 313.15 K, which is a decrease of 17.4%. The adsorbed amount of H₂O molecules increased from 66.61 ml/g to 84.21 ml/g from 273.15 K to 283.15 K. The adsorbed amount decreased from 66.61 ml/g to 84.21 ml/g at 313.15 K, and the saturated adsorbed amount decreased by 10.39%. The potential energy distributions of CH₄, CO₂ and H₂O molecules are poisson distributed. The absolute values of the most significant interaction energies were, from high to low, H₂O > CO₂ > CH₄; the increase in temperature leads to a gradual decrease in the adsorption potential corresponding to the most significant adsorption sites of CH₄, and the water molecules moved first to the adsorption site with higher interaction energy and then to the adsorption site with smaller interaction. The energy distribution curves of all three molecules, CH₄, CO₂ and H₂O, shifted to the right with increasing pressure, and with adsorption, the adsorbate moved from the preferen-

- tial adsorption site with larger interaction energy to the secondary adsorption site with smaller interaction energy.
- (2) From the probability densities of CH₄, CO₂ and H₂O adsorption processes, it can be seen that H₂O molecules are the most abundant in adsorption sites, CO₂ has the second highest content of adsorption sites, and CH₄ molecules have the lowest content of adsorption sites. The adsorption sites of the three adsorbent molecules overlap, and competition for the same adsorption site occurs during the multiple adsorption process. The temperature was increased from 273.15 K to 313.15 K. The diffusion coefficient of CH₄ molecules was increased from $0.42 \times 10^{-9} \text{ m}^2/\text{s}$ to $0.82 \times 10^{-9} \text{ m}^2/\text{s}$, that of CO₂ molecules from $1.02 \times 10^{-9} \text{ m}^2/\text{s}$ to $1.21 \times 10^{-9} \text{ m}^2/\text{s}$, and that of H₂O molecules from $1.13 \times 10^{-9} \text{ m}^2/\text{s}$ to $1.82 \times 10^{-9} \text{ m}^2/\text{s}$. The diffusion coefficients of the three gases at the same temperature have the relationship: H₂O > CO₂ > CH₄, and the activation energies of diffusion of CH₄, CO₂ and H₂O are 12.20 kJ/mol, 3.36 kJ/mol and 8.47 kJ/mol, respectively, and the diffusion of CO₂ is more likely to occur.
 - (3) CH₄ molecules are distributed in layers in the middle part of the model; CO₂ molecules are distributed in bands along the Z-axis; H₂O molecules are distributed in multiple clusters along the Z-axis. With the increase of adsorption amount and pressure, the isosteric heat of adsorption of CH₄ and CO₂ gradually decreases, and the isosteric heat of adsorption of H₂O molecules gradually increase. The non-homogeneous effect of coal body dominates the adsorption process of CH₄ and CO₂ molecules, and the H₂O-H₂O interaction gradually dominates the adsorption process of H₂O molecules. The adsorption of CH₄ and CO₂ in the coal belongs to physical adsorption, while the adsorption process of H₂O molecules is beyond the scope of physical adsorption. The absolute values of the interaction energies were in the following order: H₂O > CO₂ > CH₄, with the increase of temperature, the absolute values of the interaction energies of CH₄ and CO₂ decreased, and the absolute values of the interaction energies of H₂O increased and then decreased; with the increase of equilibrium pressure, the absolute values of the interaction energies increased. van der Waals' energy dominated the adsorption process of CH₄ and accounted for more than 99% of the total interaction energy. During CO₂ adsorption, electrostatic energy accounted for about 35.59% and van der Waals energy accounted for 64.41%. The interaction energy of H₂O adsorption was dominated by hydrogen bonding, which accounted for about 98% of the interaction energy, and supplemented by van der Waals energy, which accounted for 2% of the interaction energy. When the pressure was greater than 8 MPa, van der Waals interactions had a negative effect on adsorption.

Data availability

The datasets used and/or analyzed during the current study are available from the corresponding author upon reasonable request.

Received: 11 March 2024; Accepted: 27 September 2024

Published online: 15 October 2024

References

1. Liang, B. et al. Experimental study on isothermal adsorption of methane by granular coal and lump coal. *J. Saf. Sci. Technol.* **13**(3), 53–57 (2017).
2. Long, H. et al. Adsorption and diffusion characteristics of CH₄, CO₂, and N₂ in micropores and mesopores of bituminous coal: Molecular dynamics. *Fuel* **292**(1), 120268 (2021).
3. Long, H. et al. Molecular simulation of the competitive adsorption characteristics of CH₄, CO₂, N₂, and multicomponent gases in coal. *Powder Technol.* **385**(1) (2021).
4. Sw, A., Zja, B. & Cda, C. Molecular simulation of coal-fired plant flue gas competitive adsorption and diffusion on coal. *Fuel* **239**, 87–96 (2019).
5. Mazumder, S. & Wolf, K. H. Differential swelling and permeability change of coal in response to CO₂ injection for ECBM. *Int. J. Coal Geol.* **74** (2), 123–138 (2008).
6. Mabuza, M. & Premllal, K. Assessing impure CO₂ adsorption capacity on selected south african coals comparative study using low and high concentrated simulated flue gases. *Energy Procedia* **51**, 308–315 (2013).
7. Wu, C. Molecular simulation of flue gas and CH₄ competitive adsorption in dry and wet coal. *J. Nat. Gas Sci. Eng.* **71**, 102980 (2019).
8. Kurniawan, Y., Bhatia, S. K. & Rudolph, V. Simulation of binary mixture adsorption of methane and CO₂ at supercritical conditions in carbons. *AIChE J.* **52** (3), 957–967 (2010).
9. Zhou, W. et al. Molecular simulation of CO₂/CH₄/H₂O competitive adsorption and diffusion in brown coal. *RSC Adv.* **9** (6), 3004–3011 (2019).
10. Kong, X. G. et al. Experimental and numerical investigations on dynamic mechanical responses and failure process of gas-bearing coal under impact load. *Soil Dyn. Earthquake Eng.* **142** (2021).
11. Fuchs, W. & Sandhoff, A. G. Theory of coal pyrolysis. *Ind. Eng. Chem.*, **34**(5): 567–571 (1942).
12. Given, P. H. The distribution of hydrogen in coals and its relation to coal structure. *Fuel* **39** (2), 147–153 (1960).
13. Wisner, W. H. Reported in division of fuel chemistry. **20** (1), 122 (1975).
14. Shinn, J. H. From coal to single-stage and two stage products: a reactive model of coal structure. *Fuel* **63** (9), 1187–1196 (1984).
15. Gao, D. M. et al. Molecular simulation of gas adsorption characteristics and diffusion in micropores of lignite. *Fuel* **269**, 117443 (2020).
16. Wu, S. Y. Molecular simulation research on mechanism of coal spontaneous combustion prevention and storage of flue gas (Liaoning technical university, 2019).
17. Xiang, J. H. Structure of characterization of coals with different rank and molecular simulation of interaction between coal and CH₄/CO₂/H₂O (Taiyuan university of technology, 2013).
18. Okolo, G. N. et al. Comparing the porosity and surface areas of coal as measured by gas adsorption, mercury intrusion and SAXS techniques. *Fuel* **141**, 293–304 (2015).
19. Zhang, R. et al. Estimation and modeling of coal pore accessibility using small angle neutron scattering. *Fuel* **161**, 323–332 (2015).
20. Zheng, Z. Molecular simulations study of the structure of Shedong and the adsorption of CH₄, CO₂ and H₂O (Taiyuan university of technology, 2009).

21. Wu, W. Z. Molecular simulation study of the structure of Shendong inertinite and the interaction of CH₄, CO₂ and H₂O (Taiyuan university of technology, 2010).
22. Zhao, K. R. Molecular simulation of the interaction between Hami inertinite structure and gases of CH₄, CO₂ and H₂O (Taiyuan university of technology, 2011).
23. Li, S. G. et al. Effect of N₂/CO₂ injection pressure on CH₄ desorption in gas-bearing coal rock. *Nat. Gas Ind.* **41**(3), 80–89 (2021).
24. Xiang, J. H. et al. Molecular simulation of the CH₄/CO₂/H₂O adsorption onto the molecular structure of coal. *Sci. China Earth Sci.* **44** (7):1418–1428 (2014).
25. Kärger, J. & Valiullin, R. Mass transfer in mesoporous materials: the benefit of microscopic diffusion measurement. *Chem. Soc. Rev.* **42**(9), 4172 (2013).
26. Du, X. et al. Thermodynamics analysis of the adsorption of CH₄ and O₂ on montmorillonite. *Appl. Clay Sci.* **192**, 105631 (2020).
27. Ma, D. M., Cao, S. L. & Li, P. Comparison on adsorption and desorption thermodynamics features between shale gas and coalbed methane. *Coal Sci. Technol.* **43**(2), 64–67 (2015).
28. Chakraborty, A., Saha, B. B. & Koyama, S. On the thermodynamic modeling of the isosteric heat of adsorption and comparison with experiments. *Appl. Phys. Lett.* 89171901 (2006).
29. Xd, A. et al. Investigation into the adsorption of CO₂, N₂ and CH₄ on kaolinite clay-science Direct. *Arab. J. Chem.* **15**(3) (2021).
30. Jin, Z. X. et al. H₂O adsorption mechanism in coal basing on Monte Carlo method. *J. China Coal Soc.*, **42** (11), 2968–2974 (2017).

Acknowledgements

This work was partly supported by the National Natural Science Foundation of China (grant number 52174183), National Natural Science Foundation of China (grant number 52374203). All authors included in this section have consented to the acknowledgement.

Author contributions

Jinzhang Jia: Methodology, Supervision, Conceptualization, Funding acquisition. Yinghuan Xing: Conceptualization, Investigation, Writing- original draft, Writing-review & editing. Bin Li: Data curation, Visualization, Software. Yumo Wu: Software. Dongming Wang: Software. All authors have read and agreed to the published version of the manuscript.

Declarations

Competing interests

The authors declare no competing interests.

Additional information

Correspondence and requests for materials should be addressed to Y.X.

Reprints and permissions information is available at www.nature.com/reprints.

Publisher's note Springer Nature remains neutral with regard to jurisdictional claims in published maps and institutional affiliations.

Open Access This article is licensed under a Creative Commons Attribution-NonCommercial-NoDerivatives 4.0 International License, which permits any non-commercial use, sharing, distribution and reproduction in any medium or format, as long as you give appropriate credit to the original author(s) and the source, provide a link to the Creative Commons licence, and indicate if you modified the licensed material. You do not have permission under this licence to share adapted material derived from this article or parts of it. The images or other third party material in this article are included in the article's Creative Commons licence, unless indicated otherwise in a credit line to the material. If material is not included in the article's Creative Commons licence and your intended use is not permitted by statutory regulation or exceeds the permitted use, you will need to obtain permission directly from the copyright holder. To view a copy of this licence, visit <http://creativecommons.org/licenses/by-nc-nd/4.0/>.

© The Author(s) 2024